

We thank the two anonymous referees for their insightful comments to the manuscript and helpful suggestions for improving the presentation quality. Below, we explain how the comments and suggestions are addressed (our point-by-point responses in blue) and make note of the changes that have been made to the manuscript, attempting to take into account all the comments raised by both referees.

Referee #1

General comments:

An analysis of model results for BC in snow in the Northwestern USA from simulations with CAM5 is presented. The focus of the paper is the validation of model results based on a combination of a large number of high-quality observational data sets. As a novelty, a Positive Matrix Factorization (PMF) analysis is performed to determine biomass and fossil fuel sources of BC in the snow.

Many models produce substantial biases in simulated BC concentrations in the atmosphere in this region. An analysis of the relationship between BC in the atmosphere and deposition on snow is a very useful approach with regard to needed improvements of climate and air quality models. Unfortunately, there are several key aspects of the approach that seem problematic. In particular, the approach likely underestimates the influence of biofuel emissions in the model as explained in more detail in the following. Second, comparisons between BC concentrations in snow and air are based on unverified assumptions about correlations between these quantities.

[Response: please see our responses to the more specific comments.](#)

Specific Comments:

Page 12964, line 7 - 13: Please clarify whether sensible and latent heat fluxes are specified in calculations of atmospheric properties and land surface processes. How do amounts of snow and BC processes in snow in specified dynamics mode compare with results from the freely running model and how accurate are results? It seems that this approach has previously been used to study atmospheric processes but it is not obvious how well it works for snow and BCC.

[Response: In the specified dynamics mode, surface sensible and latent heat fluxes are specified in calculations of atmospheric properties but not the land surface processes. However, precipitation \(including rain and snow\) and BC deposition to snow are calculated in the atmospheric component of the model. With the constrained meteorological fields the model can simulate clouds, precipitation and aerosol processes better than in the freely running mode \(e.g., Ma et al., 2013\), especially, for](#)

a specific time period (as opposed to climatology). As shown in our Figure S5 (in the supplement), the CAM5 simulated snow cover fraction (SCF) has a good agreement with satellite retrievals. The three-month mean SCF for CAM5 is 50% over Northwest USA and 99% over West Canada, comparing to mean SCF from MODIS of 58% over Northwest USA and 96% over West Canada. This is the exact reason why we choose to run the model in specified dynamics mode for comparing with the field measurements made during January-March of 2013. We have now clarified more on this in the revised manuscript.

Page 12964, line 26: The yet unpublished ECLIPSE data set is not properly acknowledged. See the ECLIPSE website for details.

Response: Thank you for pointing this out. We now cite Stohl et al. (2015) in the text, as suggested by referee #2, and have added the following statement to the acknowledgment: “ECLIPSE emission data sets are available from <http://www.geiacenter.org/access>. Funding for the development of the ECLIPSE emission data set was provided by the European Union Seventh Framework Program (FP7/2007–2013) under grant agreement no. 282688 – ECLIPSE.”.

Page 12965, line 5-8: It seems highly problematic to apply the ratio of biofuel to total emissions from the old AEROCOM/GFED emission data set by Dentener et al. (2006) to the new combined ECLIPSE/GFED3 data set that is used in CAM5. This will likely lead to incorrect estimates of fossil fuel and biofuel emissions. Different emission sectors are considered in these data sets (e.g. oil and gas flaring emissions are included in the ECLIPSE data set but are not included in the AEROCOM data set). There are also substantial differences in emissions from sources that are common to both data sets. For GFED3, there is a 43% increase in emissions for boreal North America compared to GFED2 (van der Werf et al., 2010). The latter implies that biofuel emissions and contributions to BC in snow in North America are substantially underestimated with this approach, which likely explains diagnosed underestimates in BB contributions to BC in snow in CAM5 in Fig. 6, a key conclusion.

Response: First of all, we would like to clarify on a possible misunderstanding here. When apportioning the ECLIPSE emissions to fossil fuel and biofuel, we did not use fire emission data sets (i.e., GFED2 or GFED3). The difference between GFED3 and GFED2 data sets, which are both attributed to biomass burning emissions, would not directly affect the calculation of biofuel emissions and contributions since the apportionments of ECLIPSE emissions did not use GFED3 data sets. On the other hand, the 43% increase in GFED3 emissions for boreal North America that the referee pointed out does not appear in the JFM mean emissions we used in our simulation. In

the following Table R1, we compare JFM mean emissions from the different source regions/sectors between the ECLIPSE/GFED3 and IPCC-AR5/GFED2 data sets. Biomass burning (fire) emissions in North America are not so different between the two data sets, and much smaller than fossil fuel and biofuel emissions.

We agree that the additional oil and gas flaring emissions in the ECLIPSE data set would affect the apportionments. They are substantial in the Arctic (e.g., ARC) and less so in Canada (e.g., WCA and ECA), but somehow the ECLIPSE data set has even lower emissions than the AR5 data set over USA (e.g., NEU, SEU, NWU and SWU), which might partly explain the overall low bias in the modeled BCC concentrations. However, we don't have observations to evaluate against. It is also worth noting that the difference in global total JFM emissions between the two data sets (7.692 vs. 7.718 Tg yr⁻¹) is very minimal. To give a better idea on how the apportionments of FF vs. BF might affect the source attribution and facilitate a comparison with other emissions data sets, we have revised the Figure 1 to separate out BF from the BB category. The figure is shown below (Figure R1).

Table R1: January-February-March (JFM) mean emission (Tg yr⁻¹) from each source region for two different inventories (i.e., ECLIPSE/GFED3 vs. AR5/GFED2).

Source region	Fossil fuel (Tg yr ⁻¹)			Biofuel (Tg yr ⁻¹)			Biomass burning (Tg yr ⁻¹)		
	ECLIPSE	AR5	Diff	ECLIPSE	AR5	Diff	GFED3	GFED2	Diff
ARC	0.024	0.003	0.021	0.003	0.000	0.003	0.000	0.000	0.000
WCA	0.015	0.014	0.001	0.002	0.002	0.000	0.000	0.002	-0.002
ECA	0.012	0.008	0.004	0.003	0.002	0.001	0.000	0.000	0.000
LAM	0.273	0.321	-0.048	0.106	0.113	-0.007	0.051	0.206	-0.155
NEU	0.096	0.167	-0.071	0.025	0.042	-0.017	0.001	0.002	-0.001
SEU	0.055	0.082	-0.027	0.011	0.017	-0.006	0.006	0.004	0.002
NWU	0.012	0.019	-0.007	0.002	0.003	-0.001	0.000	0.000	0.000
SWU	0.027	0.047	-0.020	0.008	0.015	-0.007	0.000	0.000	0.000
EAS	1.400	1.195	0.205	0.559	0.448	0.111	0.099	0.057	0.042
SAS	0.303	0.204	0.099	0.645	0.435	0.210	0.245	0.135	0.110
SEA	0.195	0.187	0.008	0.236	0.194	0.042	0.504	0.561	-0.057
ERCA	0.582	0.734	-0.152	0.092	0.106	-0.014	0.001	0.022	-0.021
AFME	0.381	0.250	0.131	0.802	0.376	0.426	0.693	1.481	-0.788
PAN	0.030	0.037	-0.007	0.004	0.005	-0.001	0.016	0.079	-0.063
ROW	0.172	0.142	0.030	0.000	0.000	0.000	0.001	0.001	0.000
Global	3.577	3.410	0.167	2.498	1.758	0.740	1.617	2.550	-0.833

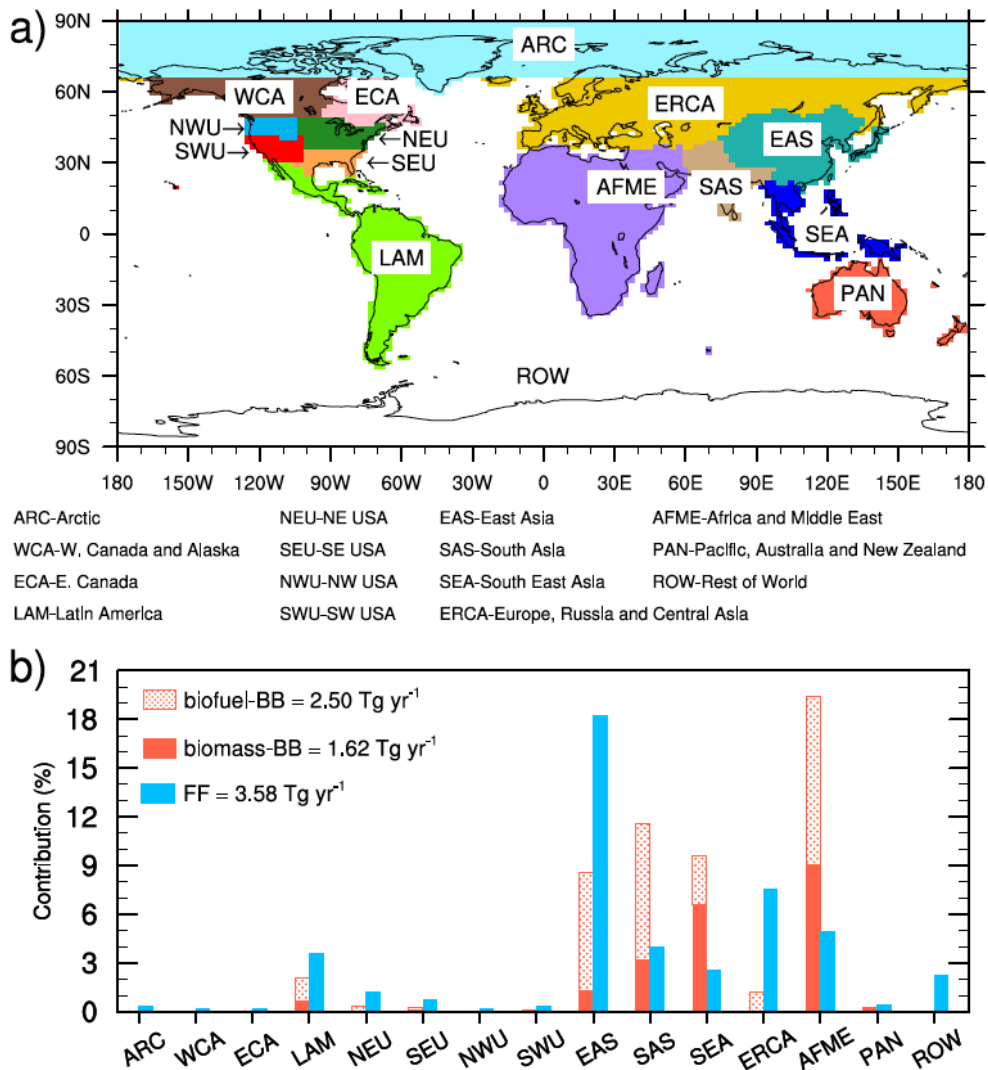


Figure R1. (a) Tagged source regions and (b) the contributions (%) to the global mean BC emissions (7.69 Tg yr⁻¹) for January, February and March from the individual source regions (marked on the horizontal axis) and sectors (FF in blue, biomass-BB in solid red, and biofuel-BB in dotted red).

Page 12968-12969: The presentation of equations and associated description of the analysis method seems somewhat lengthy and complicated. Maybe some of this could be moved to the supplement or otherwise be simplified?

Response: We agree with the referee that the equations are lengthy but they are important to calculations used in the results section. Thus we decide to move these equations in section 2.4 to the Appendix so that main text of the paper will flow better, yet readers can easily access the equations.

Page 12971-12972, section 3.2: I found it difficult to understand this section. A table of concentrations and biases in different regions would be beneficial for a more

concise summary of results.

Response: The four panels in Figure 3 visualize the model-observation comparison in different ways. We feel that the BCC concentrations and model biases have been adequately presented. Also, we mean to make the comparison for the entire regions rather than focusing on individual sites. However, following the referee's suggestion, we have made a table (Table R2), summarizing all the concentrations in Northwest USA and West Canada, and added it to the supplement as Table S3.

Table R2: BC-in-snow-column concentrations from observations and the CAM5 simulation in Northwest USA and West Canada at 36 sites

Northwest USA			West Canada		
Comparison pair i	$\overline{C_{obs}^i}$ (ng g ⁻¹)	$\overline{C_{mod}^i}$ (ng g ⁻¹)	Comparison pair i	$\overline{C_{obs}^i}$ (ng g ⁻¹)	$\overline{C_{mod}^i}$ (ng g ⁻¹)
1	8	1	21	39	44
2	15	7	22	36	18
3	25	8	23	18	19
4	31	9	24	18	13
5	29	3	25	15	7
6	52	15	26	19	6
7	78	10	27	7	4
8	88	15	28	11	13
9	62	14	29	12	16
10	45	14	30	21	22
11	35	13	31	22	29
12	28	20	32	16	25
13	34	37	33	15	9
14	17	24	34	13	20
15	19	26	35	21	27
16	18	47	36	22	30
17	73	30	mean±SD	19±8	19±11
18	110	23			
19	37	28			
20	67	40			
mean±SD	44±28	19±13			

Page 12973, lines 6-11: Comparisons between the snow column BC mixing ratio (BCC) and near-surface atmospheric concentrations of BC (BCS) are problematic for several reasons. First, at any given location, vertically integrated concentrations of BC

in the snow are largely determined by the mean deposition fluxes of BC and snow during the time period since the snow pack started to form in the fall of the previous year. If data from permanent snow fields is considered then emissions of BC from previous years may also be important. Consequently, comparisons with mean BC concentrations in air in January-February-March (JFM) should be replaced by comparisons that are based on overlapping time periods for BCC and BCS. Second, as is also pointed out in the paper, spatial variability in BC concentrations is large and cannot be fully quantified based on the relatively small number of measurement sites. The sparse distribution and lack of co-location of measurements limits the statistical robustness of the comparisons, which is not quantified. Furthermore, estimates of LMNB and LMNE are biased low in the Northwest USA region for both BCC and BCS (see previous manuscript pages). This points at a common explanation for biases in these quantities (such as an underestimate in BC emissions), opposite to the explanation given here. It is not obvious how biases in the Northwest USA region can be explained by results for Canada since the impact of local emissions on regional concentrations is so high as the study shows?

Response: None of the snow samples of Doherty et al. (2014) were of permanent snowpacks; all were from seasonal snowpacks. We agree that seasonal snowpack at our sampling sites may have started to accumulate in the fall of the previous year. However, as shown in Figure 7b of Doherty et al. (2014) there is not a vertical gradient in the mixing ratio of BC in snow at our sites. Instead there is variability, and we thought averaging across this variability would provide a more representative value for typical mixing ratios of BC in snow. The seasonality of BC emissions (i.e., biomass burning) in the cold season is also small. To address the referee's concern, we have BCC and surface-BC concentrations in four individual winter months listed in Table R3 (added to the supplement as Table S1). There is no clear trend of surface-BC and BCC variation from December to March, while for the same month surface-BC and BCC concentrations are strongly correlated. We have explained in Section 2.1 why BCC is used instead of surface-BC in the model evaluation.

Note that we are not directly comparing atmospheric concentrations (BCS) versus in snow (BCC), but rather the differences in the model biases in BCC and BCS. Regarding the sparseness of sites: We have a distribution of sampling locations across the regions for both BCC and BCS, so while the comparison is not perfect it is nonetheless of value. To address the referee's concern we have added text noting that the measures of BCC and BCS are from different locations and are not necessarily representative of the whole model grid box, so the comparison is not ideal but is nonetheless informative.

Finally, note that we do not exclude an underestimate of BC emissions as a cause of the difference; we simply also note that there is another possible cause of the low bias in BCC. We don't see a conflict here. Indeed, we make the point that any potential bias caused by model representation of BC deposition processes should show up in the comparison of BCC in both regions consistently, rather than just in the Northwest USA. Thus, we hypothesize that the difference in model bias in BCC vs. BCS is likely due mostly to an error in model emissions. The text has been edited to more clearly state this.

Table R3: CAM5 Monthly BC-in-snow-surface and BC-in-snow-column at 36 sites from December to March. ("N/A" means no snow in the model grid.)

Comparison pair <i>i</i>	BC-in-snow-surface (ng g ⁻¹)				BC-in-snow-column (ng g ⁻¹)			
	Dec	Jan	Feb	Mar	Dec	Jan	Feb	Mar
1	13	4	N/A	N/A	10	1	0	0
2	7	22	7	1	5	9	5	0
3	9	20	6	N/A	10	13	4	0
4	6	20	7	N/A	4	13	6	0
5	6	9	2	N/A	5	6	1	0
6	6	12	24	N/A	5	9	20	0
7	7	22	6	N/A	6	16	4	0
8	14	13	20	57	13	11	13	21
9	11	15	20	54	12	11	13	19
10	11	19	30	49	8	9	13	20
11	9	16	22	35	8	9	12	17
12	24	22	37	35	20	17	18	26
13	84	56	48	42	57	59	25	27
14	39	57	22	17	26	46	12	14
15	51	87	42	27	21	36	25	18
16	86	56	44	61	53	61	41	38
17	43	27	40	59	27	26	27	39
18	32	28	35	37	25	23	23	24
19	38	39	37	42	30	29	28	26
20	76	51	41	59	59	47	39	35
21	74	48	70	73	50	47	43	43
22	30	19	49	37	16	17	18	20
23	32	26	46	46	14	17	18	21
24	16	14	32	38	12	11	12	14
25	6	6	20	18	7	6	7	8
26	5	5	12	10	5	5	6	6
27	2	2	5	4	5	4	4	4
28	16	14	32	38	12	11	12	14
29	20	14	35	49	16	15	15	18

30	30	29	44	54	16	20	22	24
31	57	37	37	41	48	32	28	28
32	34	38	29	41	24	26	24	25
33	9	8	22	32	8	8	9	10
34	25	29	32	47	18	20	19	21
35	31	40	34	46	27	29	26	27
36	37	44	44	44	27	28	31	30

Page 12974, lines 7-28: Potential emissions of BC particles from soils as source of missing BC in snow in the model is an interesting topic. Soils can indeed contain microscopic particles of charcoal from vegetation fires and particles from coal combustion (Schmidt and Noack, 2000). However, various processes such as soil erosion, BC decomposition, etc. need to be considered for potential emissions of BC from soils. What concrete observational evidence exists for a soil source of measured BC snow concentrations in this study? How can the fingerprint of a soil component in the PMF analysis be explained? Soil particles and BC are both often found in snow but this does not necessarily imply a common source. For instance, deposition of soil and BC to a snow field would be positively correlated if disturbed soils and fossil fuel sources of BC are both upwind of the snow field. Further, forest fires plumes may contain soil chemical elements and can therefore also produce a positive correlation. Hence it is not clear how a lack of BC in snow can be explained by missing (direct) emissions from soils in the model.

Response: We too think this is an interesting topic and thus we explained in the text our hypothesis of the importance of soil BC in the Northwest USA domain (e.g., Schmidt and Noack, 2000; Hegarty et al., 2011). We do not have concrete and direct observational evidence of there being BC in the soil source that ends up in the snow, but infer this from the PMF analysis. The interpretation of the soil factor in the PMF analysis is based on the measured high loadings of well-known soil constituents such as Al, K, Ti, V, Ca and As (see Figure S3 in the supplement). We agree that some of these soil chemical elements may partly originate from forest fires. A PMF analysis is much more than a simple correlation analysis. The ranked, orthogonal covariance analysis tells us that the optimum variance reduction is achieved when part of the BC is in fact from a source distinct from direct fire emissions even when such emissions are present. Furthermore, this source is associated with soil markers. Hence, the PMF results do suggest a separate soil source and such a source is both plausible and consistent with the soil data for the Northwest USA region, as discussed in the text.

While the magnitude of this source of BC to snow as quantified by the PMF analysis has large uncertainties, it does suggest that this mechanism for getting BC into snow is not insignificant in some locations. We believe that wind-blown soil BC, as

opposed to atmospheric BC directly from emissions, contributes to BC measured in the snow. Importantly, as we point out, this process is not considered in the model simulation. We have now clarified more on this in the revised manuscript accordingly.

P. 12978, line 5-7: Please add more quantitative information about the differences.

What are the mean values and standard deviations?

Response: Done as suggested. The text is revised to “Compared to the original PMF values (including contributions from FF, BB and soil), CAM5 underestimates the BB contribution for 80% of the comparison pairs (modeled mean and standard deviation of $18\% \pm 5\%$ vs. PMF values of $28\% \pm 22\%$) and overestimates the FF contribution for all comparison pairs ($82\% \pm 5\%$ vs. $47\% \pm 21\%$).”

P. 12978, line 9: Define what combustion sources are considered. Does this refer to fossil fuel combustion emissions (P. 12974, line 9)?

Response: The combustion sources mentioned here include fossil fuel combustion and biofuel/biomass burning that are considered in the CAM5 simulation. This has now been clarified in the revised manuscript.

P. 12980, line 4-5. A simple linear relationship in latitudinal variations in BC radiative forcing and BC deposition flux cannot necessarily be expected and the meaning of such a relationship is not clear. For instance, the radiative forcing depends on insolation and therefore latitude, which is not considered here. In addition, as explained above, JFM deposition fluxes and concentrations are not a good proxy of the BC loading in the snow pack. Furthermore, the discussion of radiative forcings does not seem to be logically connected to discussions in the rest of the paper.

Response: We agree with the referee’s arguments here. However, both the atmospheric and in-snow BC radiative forcings were calculated interactively in the CAM5 simulation using online radiative transfer models with factors such as atmospheric and in-snow BC concentrations, latitude-dependent insolation, particle sizes and optical properties considered. No simple linear relationship between BC forcing and deposition flux was used. Such a relationship was simply meant as a first-order approximation if we were to attribute the calculated radiative forcing to the different sources. This has now been clarified in the revised manuscript. We believe the radiative forcing calculation would be of interest to colleagues who have done/are doing similar calculations for the same region and other parts of the globe. It is also useful to compare the forcing between different regions and with global mean values. Therefore, we decided to keep the discussion but we now provide some context for this in the introduction section.

Referee #2

This paper concerns a tagging technique of black carbon (BC) emissions to study the source-receptor relationship for BC in the atmosphere and on snow in Western North America using CAM5. The model results are compared with observations in the region. As most models seem to underestimate BC near the surface at high latitudes, this paper is relevant and might be of great interest to the scientific community. The questions raised in the study are within the scope of ACP. The figures are in good quality and the figure captions explain the figures well. However, for the paper to be published in ACP, some revisions need to be done. The authors should work more on the overall presentation of their results.

Specific Comments:

1. In general, I think the paper is somewhat too long and unfocused. The paper would benefit from a substantial reduction both in the Methods chapter and also the Results and Discussion. An effort to focus those parts would make the paper much easier to read. You explain your methods well, but there are still parts in Methods that can be moved to Introduction or Supplementary. For instance, the second paragraph in 2.1 Observations you discuss what is new in this study and what previous studies have done. 2.1 should only describe the actual observations, and the rest can be skipped/compressed/moved to introduction. There are many equations in 2.3 and 2.4 that can be moved to Supplementary if necessary. Also, in the Results chapter, only results should be presented (and not repetition of Methods for instance). The whole Results chapter can be shortened for clarity.

Response: Thanks for the constructive suggestions. We have now significantly revised the Methods section and the Results section following the suggestions. Section 2.1 is shortened with some necessary information moved to introduction. Some of the equations in sections 2.3 and 2.4 are lengthy but they are important to calculations used in the Results section. Thus we decide to move them to the Appendix so that they won't affect the flow of the paper but can be easily accessed by readers. Repetition of methods in the Results section has been removed.

2. The authors should explicitly state why this study is important. Also, what are the benefits of using this tagging technique instead of doing emissions perturbations? By focusing the paper and skipping parts that are not relevant, the new contribution would be easier to detect.

Response: Black carbon (BC) is believed to be an important climate-warming forcing agent in the climate system. However, the global BC forcing estimate is very uncertain, mostly because of large uncertainties in global BC emissions and

parameterizations of BC-related processes in global models. Observational and modeling studies focusing on specific regions have been useful for reducing such uncertainties. Previous BC studies, especially those addressing BC-in-snow effects, have mostly focused on polar regions and mountainous regions. The climate effect of BC might be greater in mid-latitude regions, among which North America has received less attention. The recent large-area survey of observed BC in snow in Western North America provides an opportunity for assessing how well global models predict BC concentrations in snow. These factors motivated the present study. Another important reason is that the prediction of global spatial distribution of BC by the Community Atmosphere Model (CAM5) has been significantly improved (Wang et al., 2013) and, additionally, a BC source-tagging technique was recently implemented to the model for source-attribution study (Wang et al., 2014; Zhang et al., 2015). Different global modeling approaches have been previously employed to establish aerosol source-receptor relationships, among which emissions perturbations have been widely used. Not only does this approach assume a linear response to perturbations to get fractional contribution of different sources, but it also requires additional simulations for each source perturbation. The latter would add about 30 times more computational cost than our direct tagging approach for the 32 source regions/sectors. Thus we believe the tagging technique is more computationally efficient and gives more accurate results.

We have now clarified this in the revised manuscript.

3. I am a bit confused why you separate out BF from FF and lump together with BB. The ECLIPSE emissions have different sectors compared to the previous ones from Dentener et al (2006). For instance flaring is included as a sector in ECLIPSE. There are no easy way to separate out BF, but you should at least discuss your assumptions further. What uncertainties do you introduce?

Response: The main purpose of the regrouping is to facilitate the comparison with the PMF analysis, which is able to distinguish BC from the combustion of fossil fuels versus BC from the combustion of biomass/biofuels. The chemical markers from open biomass burning (e.g. forest fires) and biofuel burning (e.g. woodsmoke from fireplaces and wood stoves) are quite similar so we could not distinguish the two in the PMF. The text has been edited to more clearly state this. We also revised Figure 1 to show BF and biomass burning contributions separately in each source region, and created a table (Table R1) to compare emissions from the different sectors between ECLIPSE/GFED3 and the popularly used IPCC AR5 data sets, which indicates that the oil and gas flaring in ECLIPSE should not significantly affect our results. Please see our response to the similar comment from referee #1.

4. Klimont et al. is still in preparation the ECLIPSE emissions data set v4a, but in the meantime Stohl et al. 2015 should be a sufficient reference: <http://www.atmoschem-phys-discuss.net/15/15155/2015/acpd-15-15155-2015.html> Here, the emissions are described in more detail.

Response: Thanks for pointing to the reference, which is now referred to in the manuscript.

5. In the results chapter; would it be an idea to not use the abbreviations for the source regions? This will make it easier to follow.

Response: We now tried to spell out the source regions frequently and make the results easier to follow.

6. The radiative forcing sub chapter was unexpected. You have not mentioned this earlier in the paper. How is the forcing calculated? How did you estimate BC DRF in the atmosphere? As a difference between surface and TOA? How do you calculate the surface RF (dimming) compared to output from SNICAR? Also, you conclude that a positive forcing at the surface (?) means heating at the surface. This is not correct, and I would avoid writing this unless you have a fully coupled climate run. Whether BC warms the surface depend on the height of BC in the atmosphere. You also find a correlation between deposition and surface RF. What about the albedo? Solar radiation? You only look at the winter months. The section in its current form seems misplaced. I suggest to either expand the analysis, or to skip this section entirely.

Response: We have now added to the introduction some background information for the BC radiative forcing calculation. Although our model simulation is not a fully coupled climate run, in which temperatures of ocean, land surface and atmosphere evolve freely, both the atmospheric and in-snow BC radiative forcings were calculated in the CAM5 simulation using online radiative transfer models (RRTMG for atmospheric radiation and SNICAR for BC in snow/ice). BC direct radiative forcing (DRF) in the atmosphere was estimated as the difference between the net radiative fluxes at the surface and TOA. Atmospheric BC has a net heating effect in the atmosphere and a net cooling effect at the surface (i.e., surface dimming). BC-in-snow effect is to increase the absorption of solar radiation in snow and, therefore, reduce the reflected radiation from the surface, representing a radiative heating effect. In the surface energy budget equation, atmospheric BC reduces downwelling shortwave radiative flux while in-snow BC reduces upwelling shortwave radiative flux. We believe there is no problem in this. However, the longwave radiative fluxes and surface sensitive/latent heat fluxes are not discussed here.

7. I'm curious about the BC in soils. How do you find this in your own analysis? I am not sure if I understood this correctly. Since this is part of your conclusions, it should be elaborated a bit more I think.

Response: BC in soil was identified by chemical “fingerprints” in the PMF analysis (Figure S3; more detailed discussion of the PMF analysis can be found in Doherty et al., 2014). Please also see our response to the similar comment raised by referee #1.

References:

- Dentener, F., Kinne, S., Bond, T., Boucher, O., Cofala, J., Generoso, S., Ginoux, P., Gong, S., Hoelzemann, J. J., Ito, A., Marelli, L., Penner, J. E., Putaud, J.-P., Textor, C., Schulz, M., van der Werf, G. R., and Wilson, J.: Emissions of primary aerosol and precursor gases in the years 2000 and 1750 prescribed data-sets for AeroCom, *Atmos. Chem. Phys.*, 6, 4321–4344, doi:10.5194/acp-6-4321-2006, 2006.
- Doherty, S. J., Dang, C., Hegg, D. A., Zhang, R., and Warren, S. G.: Black carbon and other light-absorbing particles in snow of central North America, *J. Geophys. Res.-Atmos.*, 119, doi:10.1002/2014JD022350, 2014.
- Hegarty, J., D. Zabowski, and J. D. Bakker. 2011. Use of soil properties to determine the historical extent of two western Washington prairies. *Northwest Science*, 85:120–129.
- Ma, P.-L., Rasch, P. J., Wang, H., Zhang, K., Easter, R. C., Tilmes, S., Fast, J. D., Liu, X., Yoon, J.-H., and Lamarque, J.-F.: The role of circulation features on black carbon transport into the Arctic in the Community Atmosphere Model Version 5 (CAM5), *J. Geophys. Res.-Atmos.*, 118, 4657–4669, 2013.
- Schmidt, M. W. I., and Noack, A. G.: Black carbon in soils and sediments: Analysis, distribution, implications, and current challenges, *Global Biogeochem. Cycles*, 14, 777-793, 2000.
- Stohl, A., Aamaas, B., Amann, M., Baker, L. H., Bellouin, N., Berntsen, T. K., Boucher, O., Cherian, R., Collins, W., Daskalakis, N., Dusinska, M., Eckhardt, S., Fuglestedt, J. S., Harju, M., Heyes, C., Hodnebrog, Ø., Hao, J., Im, U., Kanakidou, M., Klimont, Z., Kupiainen, K., Law, K. S., Lund, M. T., Maas, R., MacIntosh, C. R., Myhre, G., Myriokefalitakis, S., Olivie, D., Quaas, J., Quennehen, B., Raut, J.-C., Rumbold, S. T., Samset, B. H., Schulz, M., Seland, Ø., Shine, K. P., Skeie, R. B., Wang, S., Yttri, K. E., and Zhu, T.: Evaluating the climate and air quality impacts of short-lived pollutants, *Atmos. Chem. Phys. Discuss.*, 15, 15155-15241, doi:10.5194/acpd-15-15155-2015, 2015.
- van der Werf, G. R., Randerson, J. T., Giglio, L., Collatz, G. J., Mu, M., Kasibhatla, P. S., Morton, D. C., DeFries, R. S., Jin, Y., and van Leeuwen, T. T.: Global fire emissions and the contribution of deforestation, savanna, forest, agricultural, and peat fires (1997–2009), *Atmos. Chem. Phys.*, 10, 11707-11735, doi:10.5194/acp-10-11707-2010, 2010.
- Wang, H., Easter, R. C., Rasch, P. J., Wang, M., Liu, X., Ghan, S. J., Qian, Y., Yoon, J.-H., Ma, P.-L., and Vinoj, V.: Sensitivity of remote aerosol distributions to representation of cloud–aerosol interactions in a global climate model, *Geosci. Model Dev.*, 6, 765–782, doi:10.5194/gmd-6-765-2013, 2013.
- Wang, H., Rasch, P. J., Easter, R. C., Singh, B., Zhang, R., Ma, P. L., Qian, Y., and Beagley, N.: Using

an explicit emission tagging method in global modeling of source-receptor relationships for black carbon in the Arctic: Variations, Sources and Transport pathways, *J. Geophys. Res.-Atmos.*, 119, 12888–12909, doi:10.1002/2014JD022297, 2014.

Zhang, R., Wang, H., Qian, Y., Rasch, P. J., Easter, R. C., Ma, P.-L., Singh, B., Huang, J., and Fu, Q.: Quantifying sources, transport, deposition, and radiative forcing of black carbon over the Himalayas and Tibetan Plateau, *Atmos. Chem. Phys.*, 15, 6205-6223, doi:10.5194/acp-15-6205-2015, 2015.

Quantifying sources of black carbon in Western North America using observationally based analysis and an emission tagging technique in the Community Atmosphere Model

Rudong Zhang^{1,2,3}, Hailong Wang², Dean A. Hegg³, Yun Qian², Sarah J. Doherty⁴, Cheng Dang³, Po-Lun Ma², Philip J. Rasch², and Qiang Fu^{1,3}

¹ Key Laboratory for Semi-Arid Climate Change of the Ministry of Education, College of Atmospheric Sciences, Lanzhou University, Lanzhou 730000, Gansu, China.

² Atmospheric Sciences and Global Change Division, Pacific Northwest National Laboratory (PNNL), Richland, WA 99352, USA.

³ Department of Atmospheric Sciences, Box 351640, University of Washington, Seattle, WA 98195, USA.

⁴ Joint Institute for the Study of Atmosphere and Ocean, 3737 Brooklyn Ave NE, Seattle, WA 98195, USA.

Manuscript for submission to *Atmospheric Chemistry and Physics*

Correspondence to: Hailong.Wang@pnnl.gov

Abstract

1
2 The Community Atmosphere Model (CAM5), equipped with a technique to tag black carbon
3 (BC) emissions by source regions and types, has been employed to establish source-receptor
4 relationships for atmospheric BC and its deposition to snow over Western North America. The
5 CAM5 simulation was conducted with meteorological fields constrained by reanalysis for year
6 2013 when measurements of BC in both near-surface air and snow are available for model
7 evaluation. We find that CAM5 has a significant low bias in predicted mixing ratios of BC in
8 snow but only a small low bias in predicted atmospheric concentrations over the Northwest USA
9 and West Canada. Even with a strong low bias in snow mixing ratios, radiative transfer
10 calculations show that the BC-in-snow darkening effect is substantially larger than the BC
11 dimming effect at the surface by atmospheric BC. Local sources contribute more to near-surface
12 atmospheric BC and to deposition than distant sources, while the latter are more important in the
13 middle and upper troposphere where wet removal is relatively weak. Fossil fuel (FF) is the
14 dominant source type for total column BC burden over the two regions. FF is also the dominant
15 local source type for BC column burden, deposition, and near-surface BC, while for all distant
16 source regions combined the contribution of biomass/biofuel (BB) is larger than FF. An
17 observationally based Positive Matrix Factorization (PMF) analysis of the snow-impurity
18 chemistry is conducted to quantitatively evaluate the CAM5 BC source-type attribution. While
19 CAM5 is qualitatively consistent with the PMF analysis with respect to partitioning of BC
20 originating from BB and FF emissions, it significantly underestimates the relative contribution of
21 BB. In addition to a possible low bias in BB emissions used in the simulation, the model is likely
22 missing a significant source of snow darkening from local soil found in the observations.

23 1 Introduction

24 Black carbon (BC) is the most light-absorbing component of [anthropogenic](#) aerosols, and it has
25 been assessed to be responsible for a significant fraction of the climate warming in the Northern
26 Hemisphere (Bond et al., 2013). BC-containing particles impact the radiative balance of the
27 Earth-atmosphere system in several ways, including their “dimming effect” of reducing the
28 amount of radiation reaching the surface, heating the atmosphere by absorbing radiation, and a
29 darkening effect when incorporated in snow/ice at the surface, thereby increasing absorbed solar
30 radiation (Flanner et al., 2007, 2009). The latter effect is of special interest due to the strong
31 positive feedbacks it can trigger (e.g. Hansen and Nazarenko, 2004; Flanner et al., 2007; Bond et
32 al., 2013). Largely because of this latter effect, BC may play a key role in causing climate
33 change in the snow and ice covered regions of the globe, which have undergone accelerated
34 change in recent decades (Lubin and Vogelmann, 2006; Lewis et al., 2007; IPCC, 2013). There
35 have been numerous studies, both observational and modeling, attempting to highlight and
36 understand the role of BC in accelerating changes in the cryosphere (e.g., Warren and
37 Wiscombe, 1980; Clarke and Noone, 1985; Hansen and Nazarenko, 2004; Jacobson, 2004;
38 Flanner et al., 2007, 2009; Ming et al., 2008; Xu et al., 2009; Koch et al., 2009; Doherty et al.,
39 2010, 2013; Qian et al., 2011, 2015; Huang et al., 2011; Ye et al., 2012; Wang et al., 2015).
40 However, with a few notable exceptions, the focus of these studies has been either in the Polar
41 Regions or sharply circumscribed mid-latitude mountainous regions. Some recent studies (e.g.,
42 Flanner et al., 2009; Shindell and Faluvegi, 2009; Bond et al., 2013) have pointed out that the
43 climatic effect of BC might be greater at mid-latitudes, a relatively understudied region, from the
44 standpoint of global mean forcing.

45 An important aspect of the BC–climate connection is the source attribution of BC in the
46 Earth system. Such attribution is important for the formulation of mitigation strategies, a
47 particularly acute issue for BC since its relatively short lifetime holds promise for mitigation of
48 near-term climate warming. In addition, the global BC forcing estimate is very uncertain mostly
49 because of large uncertainties in BC emissions (e.g., Bond et al., 2013). Observational and
50 modeling source-attribution studies focusing on specific receptors regions are useful for
51 identifying biases in emissions. Previous source attribution studies have primarily focused on
52 sources of BC to the Arctic (e.g., Law and Stohl, 2007; Shindell et al., 2008; Hirdman et al.,
53 2010a, b; Huang et al., 2010; Jacobson, 2010; Hegg et al., 2009, 2010; Stohl, 2006; Sharma et al.,
54 2006, 2013; Sand et al., 2013; Wang et al., 2014), the Antarctic (e.g., Graf et al, 2010), or
55 various mountain regions (Fagerli et al., 2007; Kopacz et al., 2011; Lu et al., 2012; Zhang et al.,
56 2015; Wang et al., 2015). A number of studies have also suggested the importance of long-range
57 transport of aerosols to North America (e.g., Jaffe et al., 1999; VanCuren, 2003; Park et al., 2005;
58 Heald et al., 2006; Chin et al., 2007; Hadley et al., 2007; Eguchi et al., 2009; Clarke and
59 Kapustin, 2010; Fischer et al., 2010; Yu et al., 2012, 2013). A few of these studies assessed
60 transport of BC to North America from various remote source regions using numerical models.
61 For example, Hadley et al. (2007) found that long-range transport from Asia was a major source
62 of BC in the upper atmosphere over North America.

63 Recently, Wang et al. (2014) introduced an explicit aerosol tagging technique to a global
64 aerosol-climate model to produce a detailed characterization of the fate of BC in receptor regions
65 of interest emitted from various geographical source regions. Compared to other widely-used
66 approaches (e.g., the emissions perturbation approach) that have been previously employed to
67 establish global aerosol source-receptor relationships, the tagging approach neither assumes a

HW 8/11/2015 4:12 PM

Deleted: Nevertheless, a

HW 8/11/2015 4:12 PM

Deleted: them have

HW 8/11/2015 4:12 PM

Deleted: (e.g., the Arctic) emitted from various geographical source regions.

72 | linear response to perturbations to get fractional contribution of different sources, nor requires
73 | additional simulations for each source perturbation. Thus we believe the tagging technique is
74 | more computationally efficient and gives more accurate results. Zhang et al. (2015) extended the
75 | Wang et al. (2014) modeling tool so it tags source types/sectors in addition to source regions, and
76 | they conducted a BC source attribution analysis over the Himalayas and Tibetan Plateau. This
77 | modeling framework provides a powerful tool for looking at source attribution of BC in North
78 | America, an understudied mid-latitude region for BC in snow.

HW 8/11/2015 4:12 PM

Deleted: one of

HW 8/11/2015 4:12 PM

Deleted: regions, North America

79 | A key facet of employing any model such as that of Zhang et al. (2015) is an assessment
80 | of how well it actually reproduces observed values. Atmospheric observational data from the
81 | Interagency Monitoring of Protected Visual Environments (IMPROVE) long-term surface
82 | monitoring network permit an assessment of model predictions of near-surface atmospheric
83 | concentrations of BC. Observations of BC in snow in the Arctic and North China have been used
84 | to evaluate models in several previous studies (e.g., Flanner et al., 2007; Skeie et al., 2011; Wang
85 | et al., 2011; Lee et al., 2013; Jiao et al., 2014; Qian et al., 2014; Zhao et al., 2014). A recent
86 | study by Doherty et al., (2014) presented a large-area survey of observed BC concentrations in
87 | snow in Western North America (Fig. S1), affording an opportunity to make such an assessment
88 | for model predictions of BC in snow. For the first time, we use their measurements of BC in
89 | snow over North America to evaluate our global aerosol-climate model in terms of the amount
90 | and sources of BC in snow. The Doherty et al. (2014) study included a Positive Matrix
91 | Factorization (PMF) source attribution analysis of BC in snow, making feasible an additional
92 | assessment of the source attribution of BC in snow in the enhanced CAM5 model. Here we
93 | assess the CAM5 results against these observations and analyses for two receptor areas defined
94 | by the western North American region for which the Doherty et al. (2014) data are available.

HW 8/11/2015 4:12 PM

Deleted: In this regard, the recent study by Doherty et al., (2014) presented a large

HW 8/11/2015 4:12 PM

Moved (insertion) [1]

HW 8/11/2015 4:12 PM

Deleted: Additionally, data from a long-standing atmospheric observational network permits a complementary assessment of

HW 8/11/2015 4:12 PM

Deleted: predictions of near-surface atmospheric concentrations of BC. Finally, as part of the

HW 8/11/2015 4:12 PM

Deleted: ,

HW 8/11/2015 4:12 PM

Deleted: makes

106 Additionally, we present radiative transfer calculations in the atmosphere and snow with
107 the evaluated model to assess the impact of the modeled BC as well as dust on the radiative
108 balance for the studied region. This facilitates a comparison of the radiative forcing between this
109 region and other mid-latitude or high-latitude regions.

HW 8/11/2015 4:12 PM

Deleted: .

110

111 2 Methods

112 2.1 Observations

113 Monthly mean near-surface atmospheric BC concentrations for January, February and March of
114 2013 used in this study are from IMPROVE non-urban background sites within the United States
115 (Malm et al., 1994). Fine particles (PM_{2.5}, particles with aerodynamic diameters < 2.5 μm) are
116 captured on filters, which are weighed and then subjected to BC concentration analysis using the
117 thermal-optical measurement technique in a laboratory (Chow et al. 1993, 2007).

HW 8/11/2015 4:12 PM

Deleted: the Interagency Monitoring of Protected Visual Environments (IMPROVE, <http://vista.cira.colostate.edu/IMPROVE/>) long-term surface monitoring network at

118 While previous observation/model comparisons of BC in snow have typically compared
119 BC mixing ratios in the surface snow, here we compare the average snow column BC mixing
120 ratio (calculated as the sum of all BC in the snow column divided by the column equivalent
121 water mass, hereafter BCC) over a specified period of time. This is likely a better metric for
122 model comparison than the BC concentration in the top snow layer only, since surface snow
123 mixing ratios at a given point in time can be strongly affected by, e.g., how recently new snow
124 fell, accurate representation of BC mixing ratios in the most recent snowfall and other processes
125 that can vary on the timescale of days. In particular, melting of surface snow can strongly
126 enhance surface snow mixing ratios but melting followed by percolation and refreezing
127 redistributes BC particles within the snow column, resulting in no change to the total BC mass in
128 the snow column. Indeed, Doherty et al. (2014) found that BCC is more regionally consistent

HW 8/11/2015 4:12 PM

Moved up [1]: in snow in the Arctic and North China have been used to evaluate models in several previous studies (e.g., Flanner et al., 2007; Skeie et al., 2011; Wang et al., 2011; Lee et al., 2013; Jiao et al., 2014; Qian et al., 2014; Zhao et al.,

HW 8/11/2015 4:12 PM

Deleted: Observations of BC concentrations

HW 8/11/2015 4:12 PM

Deleted: 2014). For the first time, we use measurements of BC in snow over North America (Doherty et al., 2014) to evaluate our global aerosol-climate model in terms of the amount and sources of BC in snow.

HW 8/11/2015 4:12 PM

Deleted: (ideally a month or season), as suggested by Doherty et al. (2014).

147 | than BC concentrations in top snow layer. Further, they showed that while there were vertical
148 | variations in the mixing ratio of BC in snow at their study sites there is no consistent vertical
149 | gradient. This is also the case in the model Table S1 consistent with the fact that BC emissions
150 | during the cold season don't have strong temporal gradient. Hence, in this study, we use the BCC
151 | data from Table 6 of Doherty et al. (2014) to evaluate our model.

152 | The BCC estimates by Doherty et al. (2014) are based on samples of seasonal snow
153 | collected January through March 2013 at 67 sites in the northwest and north-central U.S. and
154 | Canada. Snow BC mixing ratios are estimated based on an optical measurement of spectrally-
155 | resolved light absorption by all particles in the snow, using an ISSW (Integrating
156 | Sphere/Integrating Sandwich) Spectrophotometer (Grenfell et al., 2011). Absorption is
157 | apportioned to BC and non-BC particulate components using the measured absorption Ångström
158 | exponent 450-600 nm along with assumed absorption Ångström exponents of the BC and non-
159 | BC components. Note that the absorption Ångström exponent is the slope of the logarithm of
160 | absorption versus the logarithm of wavelength. Absorption attributed to BC is then converted to
161 | a BC mass mixing ratio using a set of calibration standards with weighed amounts of synthetic
162 | BC. Full details of the analysis are given by Grenfell et al. (2011) and Doherty et al. (2014). Of
163 | relevance here is that this is not a direct measure of BC, but an estimate of mass based on
164 | measured absorption and the assumed optical properties of these absorbing components.

165 | 2.2 Model description and experimental design

166 | An explicit BC source tagging capability was developed in the Community Atmosphere Model
167 | version 5 (CAM5) by Wang et al. (2014), and they applied it to establish source-receptor
168 | relationships for BC in the Arctic and quantify source contributions from a few major
169 | geographical regions. Zhang et al. (2015) extended this tool to quantifying sources of BC in the

HW 8/11/2015 4:12 PM

Deleted: of the mixing ratio of BC in snow given

HW 8/11/2015 4:12 PM

Deleted: Snow samples were collected at a range of depths through the whole snow column at each site.

HW 8/11/2015 4:12 PM

Deleted: in each snow sample

HW 8/11/2015 4:12 PM

Deleted: 600nm

HW 8/11/2015 4:12 PM

Deleted: ..

177 Himalayas and Tibetan Plateau originating from biomass & biofuel (BB) and fossil fuel (FF)
178 sectors in various regions. In this study, we use CAM5 with this explicit BC tagging technique,
179 including a recently improved representation of convective transport and wet scavenging of
180 aerosols (H. Wang et al., 2013). We conduct a CAM5 simulation at a horizontal resolution of
181 $1.9^\circ \times 2.5^\circ$ and 56 vertical levels in the specified dynamics mode (Ma et al., 2013), in which
182 model meteorology (e.g., wind, temperature, surface pressure, surface stress, and surface fluxes)
183 are constrained to agree with the NASA Modern Era Retrospective-Analysis for Research and
184 Applications (MERRA) 6 hourly reanalysis (Rienecker et al., 2011), while atmospheric
185 constituents such as water vapor, clouds, and aerosols are allowed to evolve according to their
186 prognostic equations in the model. Although land surface processes including those involve BC
187 in snow are not directly nudged to observations, the constrained meteorological fields should
188 make modeled precipitation and BC deposition more accurate. Monthly-mean model fields for
189 January to March 2013 are used for the comparison to observations in the large-area survey of
190 BC in snow in Western North America (Doherty et al., 2014) and in the comparison to the
191 IMPROVE surface network measurements, and they are used to establish source-receptor
192 relationships and quantify BC radiative forcing.

193 Accurate BC emissions are critical to accurate modeled distributions of BC in the
194 atmosphere and snow, but BC emissions are highly uncertain (e.g., Bond et al., 2013). Instead of
195 using the Intergovernmental Panel on Climate Change (IPCC) AR5 present-day (year 2000) BC
196 inventory (e.g., Lamarque et al., 2010), we compile a new BC emission dataset of year 2010 for
197 our simulation. The 2010 BC emission dataset consists of three parts: 1) The annually-constant
198 total BC emissions over land surfaces, obtained from the ECLIPSE (Evaluating the Climate and
199 Air Quality Impacts of Short-Lived Pollutants) V4a dataset (Stohl et al., 2015), which was

HW 8/11/2015 4:12 PM

Deleted:

HW 8/11/2015 4:12 PM

Deleted: to compare with

HW 8/11/2015 4:12 PM

Deleted: ,

203 developed within the framework of the ECLIPSE European project (<http://eclipse.nilu.no>) using
204 the Greenhouse gas and Air pollution Interactions and Synergies (GAINS) model (Amann et al.,
205 2011), including BC emissions from gas flaring (Stohl et al., 2013); 2) The 2010 annually-
206 constant BC shipping emissions from the IPCC RCP6 (Representative Concentration Pathways);
207 and 3) The 2010 seasonally-varying biomass burning BC emissions from the Global Fire
208 Emission Database (GFED) version 3 (van der Werf et al., 2010). Emission datasets for all other
209 aerosol species are obtained from the IPCC AR5 emission inventories (Lamarque et al., 2010).

210 To prepare BC emissions for the source-type tagging in the CAM5 simulation, we first
211 divide the total ECLIPSE BC emissions over land surface into two types, fossil fuel and biofuel,
212 using the ratio of biofuel to the total (biofuel plus fossil fuel) in each model grid provided by
213 Dentener et al. (2006). In order to make the model source categories directly comparable to those
214 given by the PMF analysis using the observational data, we then combine the GFED biomass
215 burning emissions and ECLIPSE surface biofuel emissions to form the BB emission sector
216 (biofuel and biomass). This is because, as discussed below, the PMF is unable to distinguish
217 open burning (fires) from biofuel burning. The IPCC RCP6 shipping emissions and ECLIPSE
218 surface fossil fuel emissions are also combined to form the FF emission sector (fossil fuel).
219 Figures S2 shows the geographical distributions of JFM (Jan., Feb. and Mar.) mean BB and FF
220 BC emission rate for year 2010 dataset we compiled.

221 Following the division of source/receptor regions in Work Plan (WP 2.1) of the Task
222 Force on Hemispheric Transport of Air Pollution ([http://iek8wikis.iek.fz-](http://iek8wikis.iek.fz-juelich.de/HTAPWiki/WP2.1)
223 [juelich.de/HTAPWiki/WP2.1](http://iek8wikis.iek.fz-juelich.de/HTAPWiki/WP2.1)), we define fifteen geographical source regions (Fig. 1a) for this
224 study, including ARC (Arctic), WCA (West Canada and Alaska), ECA (East Canada), LAM
225 (Latin America), NWU (Northwest USA), NEU (Northeast USA), SWU (Southwest USA), SEU

HW 8/11/2015 4:12 PM

Deleted: Then we

227 (Southeast USA), EAS (East Asia), SAS (South Asia), SEA (Southeast Asia), ERCA (Europe,
228 Russia and Central Asia), AFME (Africa and Middle East), PAN (Pacific, Australia and New
229 Zealand), and ROW (Rest of World).

230 Figure 1b summarizes the fractional contributions to global total BC emissions by
231 different source regions and sectors. The JFM mean global total BC emission rate is 7.69 Tg yr⁻¹
232 with 53.5% (sum of the red bars) from the BB sector and 46.5% (sum of the blue bars) from the
233 FF sector. Emissions from source regions in North America (i.e., WCA, ECA, NWU, NEU,
234 SWU and SEU) are quite low compared to the emissions from the major source regions in Asia,
235 Europe and Africa.

236 2.3 Metrics

237 Here we define two metrics, following Lee et al. (2013), to quantify the deviation of the
238 simulated values from the observations.

239 (1) Log-mean normalized bias (LMNB) is defined as

$$240 \quad \text{LMNB} = \frac{\sum_{i=1}^N \log_{10}\left(\frac{C_{mod}^i}{C_{obs}^i}\right)}{N} \quad (1)$$

241 (2) Log-mean normalized error (LMNE) is defined as

$$242 \quad \text{LMNE} = \frac{\sum_{i=1}^N \left| \log_{10}\left(\frac{C_{mod}^i}{C_{obs}^i}\right) \right|}{N} \quad (2)$$

243 N is the total number of data points in a given region for model evaluation. At each point
244 i , the modeled value (C_{mod}^i) represents the grid mean, while the observed value (C_{obs}^i) is the
245 average of all point measurements taken within the model grid cell.

246

247 We also define metrics to quantify fractional contribution (C_i^{BB} and C_i^{FF}) and emission
 248 source efficiency (S_i^{BB} and S_i^{FF}), following Zhang et al. (2015), as follows:

$$249 \quad C_i^{BB} = \frac{A_i^{BB}}{\sum_{i=1}^N (A_i^{BB} + A_i^{FF})} \quad C_i^{FF} = \frac{A_i^{FF}}{\sum_{i=1}^N (A_i^{BB} + A_i^{FF})} \quad (3)$$

250 where C_i^{BB} and C_i^{FF} are fractional contributions of BB and FF emissions, respectively,
 251 originating from the source region i to a BC property A_i^{BB} and A_i^{FF} (e.g., mass mixing ratio,
 252 column burden, or deposition flux) in a specified receptor region; and

$$253 \quad S_i^{BB} = \frac{C_i^{BB}}{\left[\frac{E_i^{BB}}{\sum_{i=1}^N (E_i^{BB} + E_i^{FF})} \right]} \quad S_i^{FF} = \frac{C_i^{FF}}{\left[\frac{E_i^{FF}}{\sum_{i=1}^N (E_i^{BB} + E_i^{FF})} \right]} \quad (4)$$

254 where S_i^{BB} and S_i^{FF} are the source efficiencies of BB and FF emissions, respectively, originating
 255 from the source region i , in changing BC in a specified receptor region. E_i^{BB} and E_i^{FF} are the BB
 256 and FF emission rates, respectively, in the source region i . The summation $\sum_{i=1}^N (E_i^{BB} +$
 257 $E_i^{FF})$ represents the global total emission rate from all source regions ($N = 15$ in this study). Thus
 258 the denominator terms are the corresponding contribution of BB or FF emissions in source
 259 region i to the global total BC emissions (Fig. 1b), and the efficiencies S_i^{BB} and S_i^{FF} characterize
 260 the sensitivity of BC properties in a specified receptor region to per-unit BB and FF emissions,
 261 respectively, in source region i .

262 2.4 Data preparation for source attribution

263 In addition to BC concentrations in snow, Doherty et al. (2014) also provide a PMF analysis of
 264 the sources of light absorption by all particulates in the snow. In brief, the PMF analysis
 265 determined the set of orthogonal factors, each with an associated chemical “fingerprint”, that are
 266 associated with variations in light absorption by all particulates in snow. Each of the factors are
 267 then associated with specific source types (e.g. biomass burning, fossil fuel burning, soil, mineral

HW 8/11/2015 4:12 PM

Deleted: To quantify source-receptor relationships and the sensitivity of BC in a specified receptor region to various sources (in terms of both regions and sectors), we

HW 8/11/2015 4:12 PM

Deleted: fingerprints”

HW 8/11/2015 4:12 PM

Deleted: (e.g. BC + organic “brown carbon” + soil organics + mineral dust), and

HW 8/11/2015 4:12 PM

Deleted: these fingerprints are

276 dust, etc.) based on their chemical fingerprints. The chemical markers from open biomass
277 burning (e.g., forest fires) and biofuel burning (e.g., woodsmoke from fireplaces and wood
278 stoves) are quite similar, so biomass and biofuel sources cannot be distinguished in the PMF;
279 both sources would be included in the factor identified as “biomass burning (BB)”. In order to do
280 a comparison to CAM5, which tracks the sources of BC only, rather than all light-absorbing
281 species to snow, we re-ran the PMF analysis so it determined the sources that contribute to
282 variations in snow BC only (i.e. C_{BC}^{gst} , in Doherty et al., 2014). This PMF analysis of sources of
283 BC in snow (Fig. S3) shows a similar, though not identical, source attribution as that for all light-
284 absorbing particulates in snow (given in Doherty et al., 2014). For both, the main source sectors
285 are pollution (likely mainly fossil fuel combustion), soil, and biomass/biofuel burning. These
286 three categories account for almost all of the light absorption by BC and other particles in the
287 snow samples. The fractional contribution of the fossil fuel/pollution source is higher for BC
288 (Fig. S3) than for total particulate absorption (Doherty et al., 2014), and the fractional
289 contribution by the soil factor is lower for BC than for total particulate absorption. The issue of
290 the nature of a BC component associated with soil, which is not intuitively obvious, is discussed
291 below.

292 The estimated snow BC concentration used in the PMF analysis and the fraction of
293 absorption due to the biomass burning, pollution/fossil-fuel and soil sources (F_{BB} , F_{FF} and F_{SOIL})
294 from the PMF analysis, are given in the Table S2. The PMF analysis allows some factors to
295 contribute negative fractions to absorption, which is of course unphysical. To rationalize the data
296 for comparison with CAM5, we first set all negative fractions F_{BB} , F_{FF} and F_{SOIL} to zero, and
297 then scale the remaining fractions so that they sum to 1.0, yielding adjusted values f_{BB} , f_{FF} and
298 f_{soil} .

HW 8/11/2015 4:12 PM

Deleted: .)

HW 8/11/2015 4:12 PM

Deleted: the results from

HW 8/11/2015 4:12 PM

Deleted: BC

HW 8/11/2015 4:12 PM

Deleted: show

HW 8/11/2015 4:12 PM

Deleted: S1

304 We next calculate average fractional contributions by the BB and FF sources from the
 305 PMF analysis for each of the snow samples sites falling within a given model grid box, using Eq.
 306 (A1) in the Appendix. It is important to note that the sum of BB and FF contributions does not
 307 necessarily equal to 100%. This is, of course, because of the soil source in the PMF model, a
 308 source of BC not present in CAM5. This renders the comparison between the model (i.e.,
 309 CAM5) and observed (i.e., PMF) sources of BC imperfect, an issue that will be discussed further
 310 below. The CAM5 JFM mean fractional contributions for the BB and FF sectors in each model
 311 grid box, where observational/PMF data are available, are calculated using Eq. (A2). Note that
 312 the sum of BB and FF contributions equals to 100%.

313 Based on the above procedures, we calculate the regional average of fractional
 314 contributions from the BB and FF sectors from the PMF analysis and from the CAM5 simulation
 315 using Eqs. (A3) and (A4), respectively. In principle, another fraction corresponding to the soil
 316 contribution should also be present in Eq. (A3) for the PMF analysis. By excluding this fraction,
 317 we are essentially renormalizing our fractional contributions such that \overline{BB}_{obs} and \overline{FF}_{obs} now
 318 represent the fractions of direct combustion emissions (fossil fuel and biomass/biofuel) that can
 319 be attributed to the BB and FF sectors. This renders these fractions equivalent to those generated
 320 by CAM5 via Eq. (A4).

322 3 Results and discussion

323 3.1 Near-surface atmospheric BC concentrations

324 There are 42 non-urban IMPROVE observation sites available in the northwest of the USA
 325 (Figure S4). For comparison with model results, measurements at sites located in the same model
 326 grid box are averaged first. As a result, we obtain 30 model/observation comparison pairs. The

HW 8/11/2015 4:12 PM
 Formatted: Indent: First line: 0.5"
 HW 8/11/2015 4:12 PM
 Deleted: (Eq. 5)
 HW 8/11/2015 4:12 PM
 Deleted: .
 HW 8/11/2015 4:12 PM
 Moved down [2]: $BB_{obs}^i = \frac{\sum_{k=1}^S c_{obs}^k \times f_{BB}^k}{\sum_{k=1}^S c_{obs}^k \times (f_{BB}^k + f_{FF}^k + f_{soil}^k)}$ $FF_{obs}^i = \frac{\sum_{k=1}^S c_{obs}^k \times f_{FF}^k}{\sum_{k=1}^S c_{obs}^k \times (f_{BB}^k + f_{FF}^k + f_{soil}^k)}$
 HW 8/11/2015 4:12 PM
 Deleted: (k)
 HW 8/11/2015 4:12 PM
 Deleted: (5) .
 HW 8/11/2015 4:12 PM
 Moved down [3]: where $f_{BB}^k + f_{FF}^k + f_{soil}^k \dots$ [1]
 HW 8/11/2015 4:12 PM
 Deleted: S1). S is the total number of samp... [2]
 HW 8/11/2015 4:12 PM
 Deleted: $BB_{obs}^i + FF_{obs}^i \neq 1$.
 HW 8/11/2015 4:12 PM
 Deleted: We calculate the average observed... [3]
 HW 8/11/2015 4:12 PM
 Deleted: .
 HW 8/11/2015 4:12 PM
 Moved down [4]: .
 HW 8/11/2015 4:12 PM
 Deleted: 6
 HW 8/11/2015 4:12 PM
 Moved down [5]: .
 HW 8/11/2015 4:12 PM
 Moved down [6]: the modeled snow BC ... [4]
 HW 8/11/2015 4:12 PM
 Deleted: of BB and FF deposition, respecti... [5]
 HW 8/11/2015 4:12 PM
 Deleted: 7
 HW 8/11/2015 4:12 PM
 Deleted: 8
 HW 8/11/2015 4:12 PM
 Moved down [7]:), respectively. .
 HW 8/11/2015 4:12 PM
 Deleted: (7) .
 HW 8/11/2015 4:12 PM
 Moved down [8]: .
 HW 8/11/2015 4:12 PM
 Deleted: (8) . [6]
 HW 8/11/2015 4:12 PM
 Deleted: 8

375 following analysis is based on the JFM mean modeled and observed values for these 30
376 comparison pairs.

377 Figure 2a shows the scatter plot of simulated versus observed JFM mean near-surface BC
378 concentrations. About 57% of the ratios fall within a factor of 2. The linear correlation
379 coefficient (R) is 0.5. The statistical significance of R is at >99% confidence level ($p = 0.005$, N
380 $= 30$). The LMNB and LMNE are calculated using Eqs. (1) and (2), respectively. The CAM5
381 results over the 30 grid boxes have LMNB of -0.05, which means that the model-predicted BC
382 concentrations are smaller than observations by 11% ($=1-10^{-0.05}$) on average. The model error
383 relative to the observations is, however, more substantial. The LMNE is 0.3, which means that
384 the model predictions are, on average, within a factor of 2 ($=10^{0.3}$) of the observations. Figure 2b
385 shows statistics for the JFM near-surface BC concentrations for the IMPROVE observations and
386 CAM5 results, respectively. The model moderately under-predicts mean and median BC
387 concentrations, as expected. The maximum observed and modeled near-surface BC
388 concentrations among the sites are close, but the modeled minimum and 25th percentile values
389 are higher than observed values. The observed and modeled mean values (\pm standard deviation)
390 are $72.0 \pm 63.3 \text{ ng m}^{-3}$ and $54.8 \pm 42.5 \text{ ng m}^{-3}$, respectively. The strong spatial variation in BC over
391 these sites, indicated by the high coefficient of variation (i.e., the ratio of the standard deviation
392 to the mean – see also the spatial distributions of BC in Fig. S4), renders the comparison of these
393 mid-latitude observations with CAM5 (having a horizontal grid spacing of $1.9^\circ \times 2.5^\circ$)
394 challenging. In this light, we consider the model-observational agreement within a factor of two
395 quite reasonable.

396 **3.2 BC in snow column**

397 In addition to evaluation of BC in the atmosphere, we also evaluate the model
398 performance with respect to BC in snow. Figure 3 shows a comparison between CAM5
399 predictions of BCC and the corresponding observations of BCC from the 49 sampling sites given
400 in Table 6 of Doherty et al. (2014), where total-column snow BC could be calculated. We obtain
401 36 observation/model comparison pairs by averaging measurements made at all sites located in
402 the same model grid box. This results in 20 comparison pairs in the Northwest USA and 16 in
403 West Canada (Fig. 3d; BCC concentrations for individual pairs are summarized in Table S3).
404 Modeled BCC does not differ appreciably between January, February and March for the grid
405 boxes where we made comparisons, so we use the mean BCC across all three months (JFM) in
406 the comparison with the observation.

407 Figure 3a shows the scatter plot of the simulated JFM mean values compared to observed
408 BCC over the 36 observation/model pairs. BCC is substantially lower in the modeled snowpack
409 than in the observations. This model low bias in BCC is substantially larger than in near-surface
410 atmospheric concentrations of BC (hereafter, referred to as BCS) discussed in the previous
411 section. In addition, the linear correlation coefficient (R) for the modeled versus observed BC
412 mixing ratios in snow is 0.2, significant only at the 70% level ($p = 0.3$, $N = 36$). The CAM5 BCC
413 has a LMNB (Eq. 1) of -0.2 which means that the model-predicted BCC concentrations are lower
414 than the observations by 37% ($=1-10^{-0.2}$) on average. The LMNE (Eq. 2) in the CAM5 BCC is
415 0.3 which means that the model predictions are, on average, within a factor of 2 ($=10^{0.3}$) of the
416 observations, though as noted above the correlation between the two is poor. The observed and
417 modeled means (\pm standard deviation) for these 36 BCC values are $32.7 \pm 24.5 \text{ ng g}^{-1}$ and
418 $19.1 \pm 11.5 \text{ ng g}^{-1}$, respectively. As was the case with model comparisons for BCS, BCC has a

HW 8/11/2015 4:12 PM

Deleted: 3d).

420 large coefficient of variation (i.e., the ratio of the standard deviation to the mean), reflecting the
421 strong spatial variation of BCC in this region (Fig. 3d).

422 Figure 3b compares the simulated and observed BCC as a function of latitude. The
423 modeled JFM zonal mean of BCC over the longitude range of 93.75–123.75° W (blue line in Fig.
424 3b) shows an increasing trend with latitude in the Northwest USA and a decreasing trend in West
425 Canada. This trend is also seen in the observations in West Canada, but there is no trend in BCC
426 with latitude in the Northwest USA. The model agrees well with the observations in Canada, but
427 has generally lower concentrations of BC in snow in the U.S. (Fig 3c). The observed values of
428 BCC range between 8 and 110 ng g⁻¹ in the Northwest USA with a mean of 44 ng g⁻¹, and 7 to 39
429 ng g⁻¹ in West Canada with a mean of 19 ng g⁻¹. The correlation coefficient between the observed
430 and modeled BCC is low (R=0.1) for the Northwest USA with negligible statistical significance
431 (p = 0.6, N = 20). However, the correlation coefficient (R) is relatively high (0.7) for West
432 Canada, significant at >99% confidence level (p = 0.005, N = 16).

433 Turning next to the regionally stratified LMNB and LMNE values, for the Northwest
434 USA region, the LMNB and LMNE are -0.39 (59% low bias) and 0.47 (a factor of 3),
435 respectively, while for West Canada, LMNB and LMNE are -0.04 (9% low bias) and 0.17 (a
436 factor of 1.5), respectively. Hence, for West Canada the model bias is essentially the same for the
437 BCC as it is for the BCS (in Northwest USA) while the model error is actually appreciably less.
438 For the Northwest USA, on the other hand, the LMNE is substantially worse for BCC than it was
439 for BCS. Furthermore, most of this error is associated with a model low bias far larger than was
440 the case for BCS. Note that the measurements of BCS and BCC are from different locations and
441 are not necessarily representative of the whole model grid box, so the comparison of biases in
442 BCS and BCC is not ideal but is nonetheless informative.

443 The smaller error (LMNE) in BCC for West Canada than for BCS in the Northwest USA
444 indicates the model might also be doing a better job of predicting BCS in West Canada than in
445 the Northwest USA, but it is not possible to know this since all the BCS observations we have
446 are from sites in the USA. For the Northwest USA sites the substantially larger low bias in BCC
447 versus in BCS is quite interesting. A commonly invoked explanation for a low bias in model
448 predictions of atmospheric BC has been flawed emissions inventories. For example, Mao et al.
449 (2011) indicated that there is a large uncertainty in the emissions of BC from biomass burning in
450 western North America. However, the larger low bias in BCC compared to BCS suggests that
451 deficiencies in emissions inventories are not likely the primary explanation for the model under-
452 prediction of BCC in this instance, since a source-based bias should show up in both BCS and
453 BCC (similar source attribution of BCS and BC deposition shown in Fig. 4), assuming the model
454 representation of deposition/scavenging processes is not flawed. In fact, the small bias in model-
455 predicted BCC in West Canada indicates that the model representation of BC deposition is less
456 likely to be the primary cause of the large low bias in BCC in Northwest USA.

457 In addition to emissions or model processes errors, another possibility for the difference
458 in modeled and observed BCC is a bias¹ in the observational estimates. In a recent comparison,
459 Schwarz et al. (2012) found that estimates of the mixing ratio of BC in snow using the ISSW
460 (used in the Doherty et al., 2014 study to estimate BCC) were biased high by up to a factor of
461 three when BC is mixed with dust. While this artifact could possibly explain a portion of the
462 observed discrepancy between the model predictions and the observations, it is not fully
463 consistent with the contrast in model-observational comparisons between the Northwest USA
464 and West Canada regions. Although there is significantly less dust in the Canadian samples

¹ For simplicity and consistency we use “model bias” below to describe the difference between model results and observations, although the measurements might have a significant bias or error.

HW 8/11/2015 4:12 PM

Deleted: a viable

HW 8/11/2015 4:12 PM

Deleted: 3

467 (based on both ISSW analysis of BC/non-BC partitioning of absorption and the PMF analysis)
468 than for the Northwest USA, the amount of dust present at the West Canada sites is still
469 substantial: The PMF analysis suggests that ~17% of the light absorption is associated with dust
470 for the Canadian sites on average, and much more at some sites, whereas it's ~36% at the U.S.
471 sites. Given this, we would expect to also find a model low bias in BCC for Canada on the order
472 of half that in the Northwest U.S., e.g. LMNB of about -0.2, rather than the actual near-zero bias
473 (LMNB=-0.04). Hence, the relatively good model-observational agreement for the Canadian
474 sites makes it unlikely that measurement bias in BCC is the sole source of the discrepancy
475 between the CAM5 predications and the field observations.

476 Another possible cause of lower BCC in the model versus the observations is a missing
477 source of BC to snow in the model. The sources of BC in CAM5 are biofuel burning, biomass
478 burning and fossil fuel combustion. In the model, emissions of BC from these sources are
479 incorporated in surface snow either in snowfall (wet deposition) or by settling directly to the
480 surface snow (dry deposition). In contrast to this, the PMF analysis suggests that a significant
481 source of BC in snow is soil. At first glance this seems counter-intuitive, since soil itself does not
482 produce BC. However, in mid-latitude regions the snow is often patchy, and intermixed with
483 large areas of exposed soil. This soil can mix with the snow mechanically (e.g. by livestock; X.
484 Wang et al., 2013) or by winds, which loft the soil and deposit it to snow on scales of tens to
485 hundreds of meters (Doherty et al., 2014). These exposed soil areas are subject to BC deposition
486 throughout the year and likely accumulate a substantial reservoir of BC from a multitude of
487 sources (e.g., Schmidt and Noack, 2000; Hegarty et al., 2011). This deposited BC is then subject
488 to re-suspension via saltation and deposition on the surrounding snow, along with the soil. As
489 mentioned above, the contribution of the soil/dust source to light absorption by snow impurities

HW 8/11/2015 4:12 PM
Deleted: dust
HW 8/11/2015 4:12 PM
Deleted:

HW 8/11/2015 4:12 PM
Deleted: The
HW 8/11/2015 4:12 PM
Deleted: dry
HW 8/11/2015 4:12 PM
Deleted: .

495 for the Canadian sites is $17 \pm 5\%$. In contrast, for the U.S. sites it is $36 \pm 4\%$, consistent with the
496 thinner and more variable snow cover in the U.S. region (snow cover fraction derived from
497 satellite measurements shown in Fig. S5). While the magnitude of this source of BC to snow is
498 unknown, the PMF analysis suggests this mechanism for getting BC into snow is not
499 insignificant in some locations. Thus, soil as a source of BC to snow at the USA sites likely
500 explains a substantial portion of the low bias in modeled snow BC for sites in this region with
501 patchy snow cover, and is also likely the explanation for much of the low bias over the entire
502 data set. We turn next to an assessment of the source attribution of BC in CAM5, including a
503 comparison with the results of a PMF analysis of the North American observations of BC in
504 snow.

506 3.3 Source attribution and emission source efficiency

507 3.3.1 Modeled source-receptor relationships using CAM5

508 The direct source tagging method in CAM5 provides a straightforward means of quantifying
509 source-receptor relationships for BC reaching the receptor regions in North America originating
510 from the various source regions and types. Figures 4a and 4b show relative contributions (as
511 defined in Sect. 2.3, Eq. 3) to the JFM mean BC atmospheric column burden, deposition flux,
512 and near-surface atmospheric concentrations for two receptor regions, the Northwest USA and
513 West Canada (as outlined by white boxes in Fig. 3d). The contributions are shown explicitly for
514 all major source regions and both source types (solid bar for BB and stippled bar for FF). The
515 contributions of BB and FF from minor source regions are lumped together (black bar in Figs. 4a
516 and b). Clearly, FF sources play a primary role in determining atmospheric concentrations and
517 deposition fluxes of BC. Contributions of BB and FF from the North American sources

HW 8/11/2015 4:12 PM

~~Deleted:~~ In our view,

HW 8/11/2015 4:16 PM

~~Deleted:~~ this much larger contribution of the soil source

HW 8/11/2015 4:12 PM

~~Formatted:~~ Font color: Blue

HW 8/11/2015 4:12 PM

~~Formatted:~~ Font color: Blue

HW 8/11/2015 4:12 PM

~~Formatted:~~ Font color: Blue

HW 8/11/2015 4:12 PM

~~Formatted:~~ Font color: Blue

HW 8/11/2015 4:12 PM

~~Deleted:~~ estimated BC in patchy snow

HW 8/11/2015 4:12 PM

~~Formatted:~~ Font color: Blue

HW 8/11/2015 4:12 PM

~~Deleted:~~ could explain the much more

HW 8/11/2015 4:12 PM

~~Deleted:~~ of the model for the USA comparison relative to that

HW 8/11/2015 4:12 PM

~~Deleted:~~ Canada

526 (hereafter, for brevity, we use USA to denote four source regions NWU, NEU, SWU and SEU;
527 see Figure 1a for region definitions) increase in importance moving from total column
528 atmospheric burden to deposition fluxes and then to near-surface atmospheric concentrations of
529 BC. North American sources, especially FF sources, are definitely the major sources of BC in the
530 near-surface atmosphere and of BC deposited to the surface – i.e. to snow – as they are within or
531 close to the receptor regions. Long-range transport of BC from distant sources [in Asia and Africa](#)
532 (e.g., EAS, SAS, SEA and AFME) to North America takes place mainly in the middle and upper
533 troposphere (shown in Fig. S8); BC in this part of the atmosphere is less prone to wet removal,
534 and thus contributes more to column burden than to near-surface BC or deposition. The spatial
535 distributions of JFM mean BC column burden and deposition along with BC transport pathways
536 from various distant and domestic source regions and sectors to North America are shown in Fig.
537 S6–S11.

538 Contributions to BC atmospheric column burden from all source regions are 38% BB and
539 62% FF for the Northwest USA receptor region, and 37% BB and 63% FF for the West Canada
540 receptor region. Contributions to BC column burden from the overseas combination of EAS,
541 [\(East Asia\)](#), [SAS \(South Asia\)](#), [SEA \(Southeast Asia\)](#) and [AFME \(Africa and Middle East\)](#) to the
542 Northwest USA and West Canada receptor regions are 57% (32% BB and 25% FF) and 63% (32%
543 BB and 31% FF), respectively, among which BB from SAS and FF from EAS are the two main
544 overseas sources. Contributions to BC column burden in the receptor regions from the North
545 American source regions (USA and WCA) are 41% (5% BB and 36% FF) for the Northwest
546 USA and 34% (5% BB and 29% FF) for West Canada.

547 Relative to that for total column burden, the contribution from FF increases for deposition
548 and is even greater for near-surface atmospheric BC. Contributions from the combined source

HW 8/11/2015 4:12 PM

Deleted: .

HW 8/11/2015 4:12 PM

Deleted: .

551 regions of USA and WCA to BC deposition over two receptor regions, Northwest USA and West
552 Canada, are 77% (10% BB and 67% FF) and 81% (11% BB and 70% FF), respectively. For
553 near-surface atmospheric BC, the total FF contributions from the USA and WCA ([West Canada](#)
554 [and Alaska](#)) increase to 82% (76% from USA) and 83% (75% from WCA) over Northwest USA
555 and West Canada, respectively.

556 Figures 4c and 4d show emission source efficiency (as defined in Sect. 2.3, Eq. 4) in
557 affecting the three JFM mean BC properties in both receptor regions. We use this efficiency
558 (assuming a global mean efficiency of 1) as an index to quantify the sensitivity of BC in a
559 receptor region to a fixed mass perturbation in emissions in different source regions and sectors.
560 It is not surprising that BC in a given receptor region is most sensitive to local emissions (i.e.,
561 NWU for the Northwest USA receptor and WCA for the West Canada receptor). As was the case
562 for source attributions in Figure 4a and 4b, the emission source efficiency (Fig. 4c & 4d) of more
563 local sources is lowest for total atmospheric column burden, then increases for deposition and
564 near-surface atmospheric BC. The distant emission sources have quite low efficiencies, with
565 significant non-local contributions only for the total column burden.

566 Differences in the vertical distribution of contributions to atmospheric BC are shown in
567 more detail in Fig. 5a and 5b. Modeled vertical profiles of area-averaged BC mixing ratio and
568 liquid cloud fraction over both receptor regions are also shown, in Fig. 5c and 5d, to indicate the
569 altitude where wet scavenging of aerosols in clouds is most likely to occur. Clearly, the
570 contribution of local sources significantly decreases above 800 hPa, while distant sources
571 become progressively more important at higher altitudes (Fig. 5a & 5b). BC from distant sources
572 contribute less to wet scavenging of BC mass than they do to column burden in the two receptor
573 regions. Liquid clouds are at a maximum in the 600–800 hPa layer. Here, the BC profiles also

574 show a minimum, possibly associated with cloud scavenging of BC in the model. This layer
575 (600–800 hPa) has an intermediate local source contribution between those in the higher layers
576 and the bottom layer (800–1000 hPa). Above 400 hPa, liquid clouds and thus wet removal are
577 minimal. Below 800 hPa, below-cloud scavenging by precipitation removes BC from the air and
578 in this altitude range BC sources are mostly local. This would increase the local source
579 contribution to the total deposition flux.

580 3.3.2 Comparison of source sector attribution between CAM5 and PMF

581 Using the procedures described in Sect. 2.4, our PMF source attribution results are compared
582 with the corresponding CAM5 source attributions (Table 1). Comparisons are done for each
583 model grid box where we have a model/observation comparison pair. We reiterate that for both
584 data sets BB includes emissions from both open biomass burning and biofuel burning.

585 As discussed in Sect. 2.4, the BB and FF fractions for the PMF analysis are not precisely
586 comparable to those from CAM5 since the PMF analysis has identified an additional BC source,
587 soil, which is not included in the CAM5 simulation. This is reflected in the fact that, while the
588 sum of CAM5 BB and FF contributions equals 1, the sum of BB and FF contributions from the
589 PMF analysis are commonly less than 1. Due to the lack of soil source in CAM5 and
590 uncertainties in both measurements and emissions (e.g., spatial distribution of sources and the
591 partitioning between BB and FF sectors), it is not surprising that there are quite large
592 discrepancies between the CAM5 and PMF values for some individual comparison pairs. When
593 compared to the PMF values (which included contributions from FF, BB and soil), CAM5
594 underestimates the BB contribution for 80% of the comparison pairs (modeled mean and
595 standard deviation of 18%±5% vs. PMF values of 28%±22%) and overestimates the FF
596 contribution for all comparison pairs (82%±5% vs. 47%±21%).

HW 8/11/2015 4:12 PM

Deleted: For the BC in snow data, sufficient ancillary chemical composition data were available to permit Doherty et al. (2014) to conduct a PMF analysis of the sources of light-absorption by all particulates in the snow. As discussed in Sect. 2.4, this analysis has been redone, estimating source contributions to BC only. This enables a more consistent comparison of the PMF results with our source attribution for BC in the CAM5 simulation.

HW 8/11/2015 4:12 PM

Formatted: Indent: First line: 0.5"

HW 8/11/2015 4:12 PM

Deleted: also

HW 8/11/2015 4:12 PM

Deleted: For example, in over 90% of the cases shown here CAM5 underestimates the BB fraction relative to the PMF values but uniformly overestimates FF fractions compared to corresponding PMF values.

612 For a better quantitative PMF/CAM5 comparison, relative contributions to BC were also
613 calculated for a PMF analysis allowing for BC only from direct combustion sources, i.e., the **BB**
614 **and FF** sources of BC considered in the CAM5 simulation. Average contributions of BC from
615 combustion sources only are compared for our two receptor regions in Figure 6. The two regions
616 differ little in the partitioning of the BC between BB and FF sources, but in both regions the
617 PMF indicates a larger role by BB than does the model. The PMF model attributes 32% of the
618 BC to BB for the Northwest USA region, while for West Canada the fraction is 28%. CAM5
619 attributes 16% of **BC** in the Northwest USA to BB and 15% **to BB in** West Canada. Averaging
620 over both regions, the PMF model attributes 30% of the BC to BB while CAM5 allocates 16% to
621 this source. Compared to the PMF results, **CAM5 over-predicts the ratio of FF to BB for the**
622 North American receptor region.

623 While certainly significant, the difference in source attribution between CAM5 and the
624 factor analysis is not surprising. The factors that possibly cause the substantial model low bias in
625 BCC could potentially generate biases in the source-type attribution. In addition, uncertainties in
626 BC emission data and model treatment of BC aging/deposition processes can also be a source of
627 bias in the attribution, including but not limited to 1) the partitioning of BC emissions into fossil
628 fuel and biofuel based on the ratio provided by Dentener et al. (2006); 2) initial injection heights
629 (up to 6 km) of biomass burning emissions that directly affect BC interaction with clouds and its
630 wet deposition in CAM5; 3) treatment of the mixing of hydrophobic BC particles with
631 hygroscopic components (e.g., sulfate and organics) that is important for BC aging and wet
632 removal but does not differentiate BB or FF origin in the model. These factors, among many
633 others, along with the possible measurement bias for samples with large soil dust concentrations,

HW 8/11/2015 4:12 PM

Deleted: only

HW 8/11/2015 4:12 PM

Deleted: the

HW 8/11/2015 4:12 PM

Deleted: for the

HW 8/11/2015 4:12 PM

Deleted: the

638 could explain the difference in source-type attribution between CAM5 and the PMF analysis.
639 The data we have are not sufficient to distinguish between these possible sources of bias.

640 **3.4 Radiative forcing**

641 Figure 7 shows the CAM5 modeled JFM mean atmospheric BC all-sky shortwave direct
642 radiative forcing (DRF) at the surface (dimming effect), at the top of the atmosphere (TOA) and
643 in the atmosphere (heating effect), and it also shows the radiative forcing due to BC and mineral
644 dust in snow (darkening effect), as a function of latitude (zonally averaged over the longitude
645 band 93.75–123.75° W). The forcing due to BC is separated out from other aerosol components
646 using the radiation diagnostic calculations recently implemented in CAM5 by Ghan et al. (2012),
647 while the BC- and dust-in-snow forcing are calculated in the SNICAR (SNOW, ICe, and Aerosol
648 Radiative) model (Flanner et al., 2007), which is coupled to CAM5. The CAM5/SNICAR
649 models do include the light-absorbing effect of mineral dust particles (in addition to BC). Note
650 that the surface radiative forcing due to BC and dust in snow shown here is the total-area mean
651 forcing (i.e., zero values enter the calculation for snow-free grids during the model integration),
652 so this represents the true climate forcing (Flanner et al., 2007).

653 The DRF by BC in the atmosphere (in-atmosphere heating) decreases with latitude, as
654 does DRF at the surface (cooling). The DRF of BC at the TOA maximizes around 50° N, where
655 BC- and dust-in-snow radiative forcings also reach their maxima. To explain these variations
656 with latitude, we plot the zonal mean of JFM mean BC total column burden in Figure 7, and we
657 also plot BC and dust deposition scaled by the snow cover fraction (SCF) to weigh the
658 contribution by each grid box to the area mean forcing by BC and dust in snow. The model
659 estimate of surface SCF was first assessed and found to be in reasonable agreement with the
660 satellite retrievals (shown in Fig. S5). Clearly, the total column burden shows the same trend as

661 the DRF in the atmosphere, and the BC- and dust-in-snow radiative forcing follow the respective
662 latitudinal variations of deposition flux. This suggests that the source attribution for BC DRF in
663 the atmosphere and forcing by BC in snow could be by approximated using the source-receptor
664 relationships for BC total column burden (Fig. 4) and BC deposition (Table S4), respectively, if
665 one assumes a linear relationship between radiative forcing and BC concentrations. Note that we
666 did not use such an assumption in the radiative forcing calculation.

HW 8/11/2015 4:12 PM

Deleted: can

HW 8/11/2015 4:12 PM

Deleted: S2

HW 8/11/2015 4:12 PM

Deleted: we assume

667 The color-coded numbers in Fig. 7 correspond to the various JFM mean radiative
668 forcings averaged over the entire receptor regions, Northwest USA and West Canada. The BC
669 darkening effect on snow is significant and comparable to its DRF in the atmosphere, especially
670 in West Canada where snow covers almost the entire area (Fig. S5). It's interesting to note that
671 the BC darkening effect outweighs the BC dimming effect (i.e., cooling at the surface) and
672 warming effect on the Earth-atmosphere system (i.e., DRF at the TOA) over both of the two
673 regions. The modeled surface radiative forcing due to dust in snow is very small in these regions.
674 However, Doherty et al. (2014) found that local soil dust, which is not considered in the CAM5
675 simulation, is a significant contributor to light absorption in snow over the U.S. Northern Plains,
676 as well as at some sites in Canada. Intra-regionally transported desert dust has also been shown
677 to have a significant impact on snow in the San Juan Mountains of Colorado (e.g., Painter et al.,
678 2010, 2012) and in northwest China (X. Wang et al., 2013; Zhang et al., 2013). This suggests
679 that CAM5 and other climate models that ignore the surface radiative forcing induced by soil
680 and/or desert dust in snow may significantly underestimate the impact of light-absorbing
681 impurities on snowmelt and climate.

682

683 4 Summary and conclusions

687 In this study, the CAM5 global model, implemented with an explicit BC source tagging
688 technique, has been employed to establish source-receptor relationships for atmospheric BC and
689 its deposition to snow over a large receptor area encompassing a substantial portion of the Great
690 Plains of North America. The model meteorological fields are constrained to agree with the
691 MERRA reanalysis data sets for year 2013. Model-predicted near-surface atmospheric BC
692 concentrations and BC-in-snow concentrations in January, February and March (JFM) were
693 evaluated against atmospheric observations from the IMPROVE network and field
694 measurements from a recent large-area survey of BC (and other light-absorbing particles) in
695 snow over land (Doherty et al., 2014), respectively. We found that CAM5 had a small low bias
696 (11%) but a substantial random error (about a factor of 2) in the estimates of monthly mean near-
697 surface atmospheric BC concentrations. However, the model had a substantial error (a factor of 2)
698 and a larger negative bias (37%) in the prediction of BC-in-snow concentrations at all the snow
699 sampling sites. Analysis of the geographic variation in the bias and error in modeled BC in snow
700 versus that observed, along with the comparison of the atmospheric near-surface BC, suggests
701 that the negative model bias is more likely due to the lack of a soil source for BC in patchy snow
702 rather than an underestimate of direct combustion emissions in the model simulation. Patchy
703 snow at the U.S. sites is prone to contamination of soil dust originating from the exposed soil
704 areas. The soil dust may contain BC deposited from the atmosphere, which was not included in
705 the emission inventory for the CAM5 simulation. It is also possible that some of the difference
706 between model and observation is due to a high bias in the measurements when BC is mixed
707 with significant amounts of light-absorbing soil dust.

708 The explicit direct source tagging technique in CAM5 permits a quantitative attribution
709 of BC in receptor regions (Northwest USA and West Canada) to source regions (North American

710 or more distant emissions) and source types (fossil fuel, FF, versus biomass/biofuel, BB). In the
711 model, local sources generally contribute more to near-surface BC and deposition than distant
712 sources. However, distant sources contribute significantly to the column BC burden, especially
713 to BC in the middle and upper troposphere. At these altitudes wet removal is relatively weak, so
714 little of this BC likely reaches the surface snowpack. In the model, FF is the dominant source
715 type for total column BC over the two receptor regions. FF is also the dominant local source type
716 for BC column burden, deposition, and near-surface BC. However, for all distant source regions
717 combined the contribution of BB is larger than FF.

718 An observationally-based PMF analysis of the sources of BC to snow, based on snow
719 chemistry, is compared to the CAM5 source attribution based on source tagging. While the
720 CAM5 source attribution was biased high for the FF sector and low for the BB sector compared
721 to PMF, they both show that the contribution of the FF sector is much larger than that of the BB
722 sector. For the two receptor regions examined in this study (Northwest US and Northwest
723 Canada), the relative contribution of the BB sector was underestimated by about a factor of two
724 in CAM5 relative to that given by the PMF analysis. The quantitative difference in the source-
725 type attribution between CAM5 and PMF analysis could be due to an underestimation of North
726 American BB emissions, the lack of a soil source of BC with a high BB/FF ratio in the model,
727 model treatment of aerosol aging/deposition processes such that the wet removal rate of BC from
728 the BB sector is overestimated, and/or biases in the measurements.

729 Based on the CAM5 predictions of BC concentrations in both the air and snow, and of
730 dust in snow, radiative forcing calculations were carried out for our two North American
731 receptor regions (Figure 3d). The darkening effect of BC in surface snow (i.e., snow albedo
732 reduction due to the presence of BC) is substantially larger than the BC dimming effect (i.e.,

HW 8/11/2015 4:12 PM

Deleted: -

734 reduction in surface radiative flux due to BC in the atmosphere) but is comparable to BC heating
 735 in the atmosphere. The modeled surface radiative forcing due to dust in snow is small in the two
 736 regions. However, Doherty et al. (2014) found that local soil, which is not considered in the
 737 CAM5 simulation, is a significant contributor to light absorption in snow, suggesting that CAM5
 738 and other climate models that ignore the local soil contributions to snow may significantly
 739 underestimate the impact of light-absorbing impurities on snowmelt and climate.

740 **Appendix:**

741 The average fractional contributions by the BB and FF sources from the PMF analysis for
 742 each of the snow samples sites (k) falling within a given model grid box are calculated using Eq.
 743 (A1).

$$744 \quad BB_{obs}^i = \frac{\sum_{k=1}^S c_{obs}^k \times f_{BB}^k}{\sum_{k=1}^S c_{obs}^k \times (f_{BB}^k + f_{FF}^k + f_{soil}^k)} \quad FF_{obs}^i = \frac{\sum_{k=1}^S c_{obs}^k \times f_{FF}^k}{\sum_{k=1}^S c_{obs}^k \times (f_{BB}^k + f_{FF}^k + f_{soil}^k)} \quad (A1)$$

HW 8/11/2015 4:12 PM
 Moved (insertion) [2]

745 where $f_{BB}^k + f_{FF}^k + f_{soil}^k = 1$. C_{obs}^k is the estimated snow BC concentrations used in the PMF
 746 analysis for the snow sampling site k (Table S2). S is the total number of sampling sites within
 747 the same model grid box.

HW 8/11/2015 4:12 PM
 Moved (insertion) [3]

748 The CAM5 JFM mean fractional contributions for the BB and FF sectors in each model
 749 grid box, where observational/PMF data are available, are calculated using Eq. (A2).

$$750 \quad BB_{mod}^i = \frac{\sum_{j=1}^M c_{mod}^j \times D_{BB}^j}{\sum_{j=1}^M c_{mod}^j \times (D_{BB}^j + D_{FF}^j)} \quad FF_{mod}^i = \frac{\sum_{j=1}^M c_{mod}^j \times D_{FF}^j}{\sum_{j=1}^M c_{mod}^j \times (D_{BB}^j + D_{FF}^j)} \quad (A2)$$

HW 8/11/2015 4:12 PM
 Moved (insertion) [4]

HW 8/11/2015 4:12 PM
 Moved (insertion) [5]

751 where C_{mod}^j are the modeled snow BC concentrations in month j for the model grid box i .
 752 D_{BB}^j and D_{FF}^j are fractional contributions of BB and FF deposition, respectively, to total BC
 753 deposition in month j , and $D_{BB}^j + D_{FF}^j = 1$. M is 3 (total number of months).

HW 8/11/2015 4:12 PM
 Moved (insertion) [6]

The regional average of fractional contributions from the BB and FF sectors from the PMF analysis and from the CAM5 simulation is calculated using Eqs. (A3) and (A4), respectively.

$$\overline{BB}_{obs} = \frac{\sum_{n=1}^N \overline{C}_{obs}^n \times BB_{obs}^n}{\sum_{n=1}^N \overline{C}_{obs}^n \times (BB_{obs}^n + FF_{obs}^n)} \quad \overline{FF}_{obs} = \frac{\sum_{n=1}^N \overline{C}_{obs}^n \times FF_{obs}^n}{\sum_{n=1}^N \overline{C}_{obs}^n \times (BB_{obs}^n + FF_{obs}^n)} \quad (A3)$$

$$\overline{BB}_{mod} = \frac{\sum_{n=1}^N \overline{C}_{mod}^n \times BB_{mod}^n}{\sum_{n=1}^N \overline{C}_{mod}^n \times (BB_{mod}^n + FF_{mod}^n)} \quad \overline{FF}_{mod} = \frac{\sum_{n=1}^N \overline{C}_{mod}^n \times FF_{mod}^n}{\sum_{n=1}^N \overline{C}_{mod}^n \times (BB_{mod}^n + FF_{mod}^n)} \quad (A4)$$

where N is the total number of observation/model comparison pairs (n) in a given region.

Acknowledgments. This research is based on work supported by the U.S. Department of Energy (DOE), Office of Science, Biological and Environmental Research as part of the Earth System Modeling Program. The Pacific Northwest National Laboratory (PNNL) is operated for DOE by Battelle Memorial Institute under contract DE-AC05-76RLO1830. The CESM project is supported by the National Science Foundation and the DOE Office of Science. D. A. Hegg, S. J. Doherty, C. Dang, and Q. Fu acknowledge support from the EPA STAR grant RD-82503801. R. Zhang acknowledges support from the China Scholarship Fund. We gratefully thank Stephen G. Warren for helpful advice and discussion on using the snow impurity data. [ECLIPSE emission data sets are available from http://www.geiacenter.org/access](http://www.geiacenter.org/access). [Funding for the development of the ECLIPSE emission data set was provided by the European Union Seventh Framework Program \(FP7/2007–2013\) under grant agreement no. 282688 – ECLIPSE.](#) The IMPROVE network data were made available at <http://vista.cira.colostate.edu/improve/>. Computational resources were provided by the National Energy Research Scientific Computing Center (NERSC), a national scientific user facility located at Lawrence Berkeley National Laboratory in Berkeley, California.

HW 8/11/2015 4:12 PM
Moved (insertion) [7]

HW 8/11/2015 4:12 PM
Moved (insertion) [8]

HW 8/11/2015 4:12 PM

Deleted: , and ECLIPSE BC emission dataset available at http://eccad.sedoo.fr/eccad_extract_interface/JSF/pa ge_login.jsf.

780 NERSC is the flagship scientific computing facility for the Office of Science in DOE. A portion of the
781 research was performed using DOE EMSL Molecular Sciences Computing resources located at PNNL.

782 **References**

- 783 Amann, M., Bertok, I., Borcken-Kleefeld, J., Cofala, J., Heyes, C., Höglund-Isaksson, L., Klimont, Z., Nguyen, B.,
784 Posch, M., Rafaj, P., Sandler, R., Schöpp, W., Wagner, F., and Winiwarter, W.: Cost-effective control of
785 air quality and greenhouse gases in Europe: Modeling and policy applications, *Environ. Model. Softw.*, 26,
786 1489–1501, 2011.
- 787 Bond, T. C., Doherty, S. J., Fahey, D. W., Forster, P. M., Berntsen, T., DeAngelo, B. J., Flanner, M. G., Ghan, S.,
788 Kärcher, B., Koch, D., Kinne, S., Kondo, Y., Quinn, P. K., Sarofim, M. C., Schultz, M. G., Schulz, M.,
789 Venkataraman, C., Zhang, H., Zhang, S., Bellouin, N., Guttikunda, S. K., Hopke, P. K., Jacobson, M. Z.,
790 Kaiser, J. W., Klimont, Z., Lohmann, U., Schwarz, J. P., Shindell, D., Storelvmo, T., Warren, S. G., and
791 Zender, C. S.: Bounding the role of black carbon in the climate system: A scientific assessment, *J.*
792 *Geophys. Res.-Atmos.*, 118, 5380–5552, doi:10.1002/jgrd.50171, 2013.
- 793 Chin, M., Diehl, T., Ginoux, P., and Malm, W.: Intercontinental transport of pollution and dust aerosols:
794 implications for regional air quality, *Atmos. Chem. Phys.*, 7, 5501–5517, doi:10.5194/acp-7-5501-2007,
795 2007.
- 796 Chow, J. C., Watson, J. G., Pritchett, L. C., Pierson, W. R., Frazier, C. A., and Purcell, R. G.: The DRI
797 Thermal/Optical Reflectance carbon analysis system: Description, evaluation and applications in US air
798 quality studies, *Atmos. Environ.*, 27A(8), 1185–1201, 1993.
- 799 Chow, J. C., Watson, J. G., Chen, L.-W. A., Chang, M. C. O., Robinson, N. F., Trimble, D., and Kohl, S. D.: The
800 IMPROVE_A temperature protocol for thermal/optical carbon analysis: Maintaining consistency with a
801 long-term database, *J. Air Waste Manage. Assoc.*, 57(9), 1014–1023, 2007.
- 802 Clarke, A. D., and Noone, K. J.: Soot in Arctic snow: a cause for perturbations of radiative transfer. *Atmos.*
803 *Environ.*, 19, 2045–2053, 1985.
- 804 Clarke, A., and Kapustin V.: Hemispheric aerosol vertical profiles: Anthropogenic impacts on optical depth and
805 cloud nuclei, *Science*, 329, 1488–1492, 2010.
- 806 Dang, C., and Hegg D. A.: Quantifying light absorption by organic carbon in Western North American snow by
807 serial chemical extractions, *J. Geophys. Res. Atmos.*, 119, 10,247–10,261, doi:10.1002/2014JD022156,
808 2014.
- 809 Dentener, F., Kinne, S., Bond, T., Boucher, O., Cofala, J., Generoso, S., Ginoux, P., Gong, S., Hoelzemann, J. J., Ito,
810 A., Marelli, L., Penner, J. E., Putaud, J.-P., Textor, C., Schulz, M., van der Werf, G. R., and Wilson, J.:
811 Emissions of primary aerosol and precursor gases in the years 2000 and 1750 prescribed data-sets for
812 AeroCom, *Atmos. Chem. Phys.*, 6, 4321–4344, doi:10.5194/acp-6-4321-2006, 2006.
- 813 Doherty, S. J., Warren, S. G., Grenfell, T. C., Clarke, A. D., and Brandt, R. E.: Light-absorbing impurities in Arctic
814 snow, *Atmos. Chem. Phys.*, 10, 11647–11680, doi:10.5194/acp-10-11647-2010, 2010.
- 815 Doherty, S. J., Grenfell, T. C., Forsström, S., Hegg, D. L., Brandt, R. E., and Warren, S. G.: Observed vertical
816 redistribution of black carbon and other insoluble light-absorbing particles in melting snow, *J. Geophys.*
817 *Res.-Atmos.*, 118, 5553–5569, doi:10.1002/jgrd.50235, 2013.
- 818 Doherty, S. J., Dang C., Hegg D. A., Zhang R., and Warren S. G.: Black carbon and other light-absorbing particles
819 in snow of central North America, *J. Geophys. Res.-Atmos.*, 119, doi:10.1002/2014JD022350, 2014.

- 820 Eguchi, K., Uno, I., Yumimoto, K., Takemura, T., Shimizu, A., Sugimoto, N., and Liu, Z.: Trans-pacific dust
821 transport: integrated analysis of NASA/CALIPSO and a global aerosol transport model, *Atmos. Chem.*
822 *Phys.*, 9, 3137-3145, doi:10.5194/acp-9-3137-2009, 2009.
- 823 Fagerli, H., Legrand, M., Preunkert, S., Vestreng, V., Simpson, D., and Cerqueira, M.: Modeling historical long-
824 term trends of sulfate, ammonium, and elemental carbon over Europe: A comparison with ice core records
825 in the Alps, *J. Geophys. Res.-Atmos.*, 112, D23s13, doi:10.1029/2006jd008044, 2007.
- 826 Fischer, E. V., Jaffe, D. A., Marley, N. A., Gaffney, J. S., and Marchany-Rivera, A.: Optical properties of aged
827 Asian aerosols observed over the US Pacific Northwest, *J. Geophys. Res.*, 115, D20209,
828 doi:10.1029/2010JD013943, 2010.
- 829 Flanner, M. G., Zender, C. S., Randerson, J. T., and Rasch, P. J.: Present day climate forcing and response from
830 black carbon in snow, *J. Geophys. Res.*, 112, D11202, doi:10.1029/2006JD008003, 2007.
- 831 Flanner, M. G., Zender, C. S., Hess, P. G., Mahowald, N. M., Painter, T. H., Ramanathan, V., and Rasch, P. J.:
832 Springtime warming and reduced snow cover from carbonaceous particles, *Atmos. Chem. Phys.*, 9, 2481–
833 2497, doi:10.5194/acp-9-2481-2009, 2009.
- 834 Ghan, S. J., Liu, X., Easter, R. C., Zaveri, R., Rasch, P. J., Yoon, J.-H. and Eaton, B.: Toward a minimal
835 representation of aerosols in climate models: Comparative decomposition of aerosol direct, semi-direct and
836 indirect radiative forcing, *J. Climate*, 25, 6461–6476, doi:10.1175/JCLI-D-11-00650.1, 2012.
- 837 Graf, H.-F., Shirsat, S. V., Oppenheimer, C., Jarvis, M. J., Podzun, R., and Jacob, D.: Continental scale Antarctic
838 deposition of sulphur and black carbon from anthropogenic and volcanic sources, *Atmos. Chem. Phys.*, 10,
839 2457–2465, doi:10.5194/acp-10-2457-2010, 2010.
- 840 Grenfell, T. C., Doherty, S. J., Clarke, A. D., and Warren, S. G.: Light absorption from particulate impurities in
841 snow and ice determined by spectrophotometric analysis of filters, *Appl. Opt.*, 50, 2037–2048, 2011.
- 842 Hadley, O. L., Ramanathan, V., Carmichael, G. R., Tang, Y., Corrigan, C. E., Roberts, G. C., and Mauger, G. S.:
843 Trans-Pacific transport of black carbon and fine aerosols ($D < 2.5 \mu\text{m}$) into North America, *J. Geophys.*
844 *Res.*, 112, D05309, doi:10.1029/2006JD007632, 2007.
- 845 Hansen, J. and Nazarenko, L.: Soot climate forcing via snow and ice albedos, *P. Natl. Acad. Sci. USA*, 101, 423–
846 428, doi:10.1073/pnas.2237157100, 2004.
- 847 Heald, C. L., Jacob, D. J., Park, R. J., Alexander, B., Fairlie, T. D., Yantosca, R. M., and Chu, D. A.: Transpacific
848 transport of Asian anthropogenic aerosols and its impact on surface air quality in the United States, *J.*
849 *Geophys. Res.-Atmos.*, 111, 13, D14310, doi:10.1029/2005JD006847, 2006.
- 850 [Hegarty, J. D., Zabowski, and J. D. Bakker. 2011. Use of soil properties to determine the historical extent of two
851 western Washington prairies. *Northwest Science*, 85:120–129.](#)
- 852 Hegg, D. A., Warren, S. G., Grenfell, T. C., Doherty, S. J., Larson, T. V., and Clarke, A. D.: Source Attribution of
853 Black Carbon in Arctic Snow, *Environ. Sci. Technol.*, 43, 4016–4021, doi:10.1021/es803623f, 2009.
- 854 Hegg, D. A., Warren, S. G., Grenfell, T. C., Doherty, S. J., and Clarke, A. D.: Sources of light-absorbing aerosol in
855 arctic snow and their seasonal variation, *Atmos. Chem. Phys.*, 10, 10923–10938, doi:10.5194/acp-10-
856 10923-2010, 2010.
- 857 Hirdman, D., Burkhardt, J. F., Sodemann, H., Eckhardt, S., Jefferson, A., Quinn, P. K., Sharma, S., Ström, J., and
858 Stohl, A.: Long term trends of black carbon and sulphate aerosol in the Arctic: changes in atmospheric
859 transport and source region emissions, *Atmos. Chem. Phys.*, 10, 9351–9368, doi:10.5194/acp-10-9351-
860 2010, 2010a.
- 861 Hirdman, D., Sodemann, H., Eckhardt, S., Burkhardt, J. F., Jefferson, A., Mefford, T., Quinn, P. K., Sharma, S.,
862 Ström, J., and Stohl, A.: Source identification of short-lived air pollutants in the Arctic using statistical

863 analysis of measurement data and particle dispersion model output, *Atmos. Chem. Phys.*, 10, 669–693,
864 doi:10.5194/acp-10-669-2010, 2010b.

865 Huang, J., Fu, Q., Zhang, W., Wang, X., Zhang, R., Ye, H., and Warren, S. G.: Dust and black carbon in seasonal
866 snow across Northern China, *Bull. Am. Meteorol. Soc.*, 92, 175–181, doi:10.1175/2010BAMS3064.1, 2011.

867 Huang, L., Gong, S. L., Jia, C. Q., and Lavoue, D.: Relative contributions of anthropogenic emissions to black
868 carbon aerosol in the Arctic, *J. Geophys. Res.-Atmos.*, 115, D19208, doi:10.1029/2009jd013592, 2010.

869 IPCC: Summary for Policymakers. In: *Climate Change 2013: The Physical Science Basis. Contribution of Working*
870 *Group I to the Fifth Assessment Report of the Intergovernmental Panel on Climate Change*, edited by
871 Stocker, T.F., Qin D., Plattner G.-K., Tignor M., Allen S.K., Boschung J., Nauels A., Xia Y., Bex V., and
872 Midgley P.M., Cambridge University Press, Cambridge, United Kingdom and New York, NY, USA, 2013.

873 Jacobson, M. Z.: Climate response of fossil fuel and biofuel soot, accounting for soot’s feedback to snow and sea ice
874 albedo and emissivity, *J. Geophys. Res.*, 109, D21201, doi:10.1029/2004JD004945, 2004.

875 Jacobson, M. Z.: Short-term effects of controlling fossil-fuel soot, biofuel soot and gases, and methane on climate,
876 Arctic ice, and air pollution health, *J. Geophys. Res.-Atmos.*, 115, D14209, doi:10.1029/2009jd013795,
877 2010.

878 Jaffe, D., Anderson, T., Covert, D., Kotchenruther, R., Trost, B., Danielson, J., Simpson, W., Berntsen, T.,
879 Karlsdottir, S., Blake, D., Harris, J., Carmichael, G., and Uno, I.: Transport of Asian air pollution to North
880 America, *Geophys. Res. Lett.*, 26(6), 711–714, 1999.

881 Jiao, C., Flanner, M. G., Balkanski, Y., Bauer, S. E., Bellouin, N., Berntsen, T. K., Bian, H., Carslaw, K. S.,
882 Chin, M., De Luca, N., Diehl, T., Ghan, S. J., Iversen, T., Kirkevåg, A., Koch, D., Liu, X., Mann, G. W.,
883 Penner, J. E., Pitari, G., Schulz, M., Seland, Ø., Skeie, R. B., Steenrod, S. D., Stier, P., Takemura, T.,
884 Tsigaridis, K., van Noije, T., Yun, Y., and Zhang, K.: An AeroCom assessment of black carbon in Arctic
885 snow and sea ice, *Atmos. Chem. Phys.*, 14, 2399–2417, doi:10.5194/acp-14-2399-2014, 2014.

886 Koch, D., Schulz, M., Kinne, S., McNaughton, C., Spackman, J. R., Balkanski, Y., Bauer, S., Berntsen, T., Bond, T.
887 C., Boucher, O., Chin, M., Clarke, A., De Luca, N., Dentener, F., Diehl, T., Dubovik, O., Easter, R., Fahey,
888 D. W., Feichter, J., Fillmore, D., Freitag, S., Ghan, S., Ginoux, P., Gong, S., Horowitz, L., Iversen, T.,
889 Kirkevåg, A., Klimont, Z., Kondo, Y., Krol, M., Liu, X., Miller, R., Montanaro, V., Moteki, N., Myhre, G.,
890 Penner, J. E., Perlwitz, J., Pitari, G., Reddy, S., Sahu, L., Sakamoto, H., Schuster, G., Schwarz, J. P., Seland,
891 Ø., Stier, P., Takegawa, N., Takemura, T., Textor, C., van Aardenne, J. A., and Zhao, Y.: Evaluation of
892 black carbon estimations in global aerosol models, *Atmos. Chem. Phys.*, 9, 9001–9026, doi:10.5194/acp-9-
893 9001-2009, 2009.

894 Kopacz, M., Mauzerall, D. L., Wang, J., Leibensperger, E. M., Henze, D. K., and Singh, K.: Origin and radiative
895 forcing of black carbon transported to the Himalayas and Tibetan Plateau, *Atmos. Chem. Phys.*, 11, 2837–
896 2852, doi:10.5194/acp-11-2837-2011, 2011.

897 Lamarque, J.-F., Bond, T. C., Eyring, V., Granier, C., Heil, A., Klimont, Z., Lee, D., Liousse, C., Mieville, A.,
898 Owen, B., Schultz, M. G., Shindell, D., Smith, S. J., Stehfest, E., Van Aardenne, J., Cooper, O. R.,
899 Kainuma, M., Mahowald, N., McConnell, J. R., Naik, V., Riahi, K., and van Vuuren, D. P.: Historical
900 (1850–2000) gridded anthropogenic and biomass burning emissions of reactive gases and aerosols:
901 methodology and application, *Atmos. Chem. Phys.*, 10, 7017–7039, doi:10.5194/acp-10-7017-2010, 2010.

902 Law, K. S. and Stohl, A.: Arctic air pollution: Origins and impacts, *Science*, 315, 1537–1540, 2007.

903 Lee, Y. H., Lamarque, J.-F., Flanner, M. G., Jiao, C., Shindell, D. T., Berntsen, T., Bisiaux, M. M., Cao, J.,
904 Collins, W. J., Curran, M., Edwards, R., Faluvegi, G., Ghan, S., Horowitz, L. W., McConnell, J. R.,
905 Ming, J., Myhre, G., Nagashima, T., Naik, V., Rumbold, S. T., Skeie, R. B., Sudo, K., Takemura, T.,
906 Thevenon, F., Xu, B., and Yoon, J.-H.: Evaluation of preindustrial to present-day black carbon and its

- 907 albedo forcing from Atmospheric Chemistry and Climate Model Intercomparison Project (ACCMIP),
908 Atmos. Chem. Phys., 13, 2607-2634, doi:10.5194/acp-13-2607-2013, 2013.
- 909 Levis, S., Bonan, G. B., and Lawrence, P. J.: Present-day springtime high-latitude surface albedo as a predictor of
910 simulated climate sensitivity, Geophys. Res. Lett., 34, L17703, doi:10.1029/2007GL030775, 2007.
- 911 Lu, Z., Streets, D. G., Zhang, Q., and Wang, S.: A novel back-trajectory analysis of the origin of black carbon
912 transported to the Himalayas and Tibetan Plateau during 1996–2010, Geophys. Res. Lett., 39, L01809,
913 doi:10.1029/2011GL049903, 2012.
- 914 Lubin, D. and Vogelmann, A. M.: A climatologically significant aerosol longwave indirect effect in the Arctic,
915 Nature, 439, 453–456, doi:10.1038/nature04449, 2006.
- 916 Ma, P.-L., Rasch, P. J., Wang, H., Zhang, K., Easter, R. C., Tilmes, S., Fast, J. D., Liu, X., Yoon, J.-H., and
917 Lamarque, J.-F.: The role of circulation features on black carbon transport into the Arctic in the
918 Community Atmosphere Model Version 5 (CAM5), J. Geophys. Res.-Atmos., 118, 4657–4669, 2013.
- 919 Mao, Y. H., Li, Q. B., Zhang, L., Chen, Y., Randerson, J. T., Chen, D., and Liou, K. N.: Biomass burning
920 contribution to black carbon in the Western United States Mountain Ranges, Atmos. Chem. Phys., 11,
921 11253-11266, doi:10.5194/acp-11-11253-2011, 2011.
- 922 Malm, W. C., Sisler, J. F., Huffman, D., Eldred, R. A., and Cahill, T. A.: Spatial and seasonal trends in particle
923 concentration and optical extinction in the United States, J. Geophys. Res., 99(D1), 1347–1370, 1994.
- 924 Ming, J., Cachier, H., Xiao, C., Qin, D., Kang, S., Hou, S., and Xu, J.: Black carbon record based on a shallow
925 Himalayan ice core and its climatic implications, Atmos. Chem. Phys., 8, 1343–1352, doi:10.5194/acp-8-
926 1343-2008, 2008.
- 927 Painter, T. H., Deems, J. S., Belnap, J., Hamlet, A. F., Landry, C. C., and Udall, B.: Response of Colorado River
928 runoff to dust radiative forcing in snow, P. Natl. Acad. Sci., 107, 17125–17130,
929 doi:10.1073/pnas.0913139107, 2010.
- 930 Painter, T. H., Skiles, S. M., Deems, J. S., Bryant, A. C., and Landry, C. C.: Dust radiative forcing in snow of the
931 Upper Colorado River Basin: 1. A 6 year record of energy balance, radiation, and dust concentrations,
932 Water Resour. Res., 48, W07521, doi:10.1029/2012WR011985, 2012.
- 933 Park, R. J., Jacob, D. J., Palmer, P. I., Clarke, A. D., Weber, R. J., Zondlo, M. A., Eisele, F. L., Bandy, A. R.,
934 Thornton, D. C., Sachse, G. W., and Bond, T. C.: Export efficiency of black carbon aerosol in continental
935 outflow: Global implications, J. Geophys. Res.-Atmos., 110, D11205, doi:10.1029/2004JD005432, 2005.
- 936 Qian, Y., Flanner, M. G., Leung, L. R., and Wang, W.: Sensitivity studies on the impacts of Tibetan Plateau
937 snowpack pollution on the Asian hydrological cycle and monsoon climate, Atmos. Chem. Phys., 11, 1929-
938 1948, doi:10.5194/acp-11-1929-2011, 2011.
- 939 Qian, Y., Wang H., Zhang R., Flanner M. G., and Rasch P. J.: A sensitivity study on modeling black carbon in snow
940 and its radiative forcing over the Arctic and Northern China, Environ. Res. Lett., 9, 064001,
941 doi:10.1088/1748-9326/9/6/064001, 2014.
- 942 Qian, Y., Yasunari, T. J., Doherty, S. J., Flanner, M. G., Lau, W. K., Ming, J., Wang, H., Wang, M., Warren, S. G.,
943 and Zhang, R.: Light-absorbing particles in snow and ice: Measurement and modeling of climatic and
944 hydrological impact, Adv. Atmos. Sci., 32, 64–91, 2015.
- 945 Rienecker, M. M., Suarez, M. J., Gelaro, R., Todling, R., Bacmeister, J., Liu, E., Bosilovich, M. G., Schubert, S. D.,
946 Takacs, L., Kim, G.-K., Bloom, S., Chen, J., Collins, D., Conaty, A., da Silva, A., Gu, W., Joiner, J., Koster,
947 R. D., Lucchesi, R., and Molod, A.: MERRA – NASA’s Modern-Era Retrospective Analysis for Research
948 and Applications, J. Clim., 24, 3624–3648, 2011.

- 949 Sand, M., Berntsen, T. K., Seland, Ø., and Kristjansson, J. E.: Arctic surface temperature change to emissions of
 950 black carbon within Arctic or midlatitudes, *J. Geophys. Res.*, 118, 7788–7798, doi:10.1002/jgrd.50613,
 951 2013.
- 952 [Schmidt, M. W. I., and Noack, A. G.: Black carbon in soils and sediments: Analysis, distribution, implications, and](#)
 953 [current challenges. *Global Biogeochem. Cycles*, 14, 777-793, 2000.](#)
- 954 Schwarz, J. P., Doherty, S. J., Li, F., Ruggiero, S. T., Tanner, C. E., Perring, A. E., Gao, R. S., and Fahey, D. W.:
 955 Assessing Single Particle Soot Photometer and Integrating Sphere/Integrating Sandwich Spectrophotometer
 956 measurement techniques for quantifying black carbon concentration in snow, *Atmos. Meas. Tech.*, 5, 2581–
 957 2592, doi:10.5194/amt-5-2581-2012, 2012.
- 958 Sharma, S., Andrews, E., Barrie, L. A., Ogren, J. A., and Lavoue, D.: Variations and sources of the equivalent black
 959 carbon in the high Arctic revealed by long-term observations at Alert and Barrow: 1989–2003, *J. Geophys.*
 960 *Res.*, 111, D14208, doi:10.1029/2005JD006581, 2006.
- 961 Sharma S., Ishizawa, M., Chan, D., Lavoué, D., Andrews, E., Eleftheriadis, K., and Maksyutov, S.: 16-year
 962 simulation of Arctic black carbon: Transport, source contribution, and sensitivity analysis on deposition, *J.*
 963 *Geophys. Res. Atmos.*, 118, 943–964, doi:10.1029/2012JD017774, 2013.
- 964 Shindell, D. T., Chin, M., Dentener, F., Doherty, R. M., Faluvegi, G., Fiore, A. M., Hess, P., Koch, D. M.,
 965 MacKenzie, I. A., Sanderson, M. G., Schultz, M. G., Schulz, M., Stevenson, D. S., Teich, H., Textor, C.,
 966 Wild, O., Bergmann, D. J., Bey, I., Bian, H., Cuvelier, C., Duncan, B. N., Folberth, G., Horowitz, L. W.,
 967 Jonson, J., Kaminski, J. W., Marmer, E., Park, R., Pringle, K. J., Schroeder, S., Szopa, S., Takemura, T.,
 968 Zeng, G., Keating, T. J., and Zuber, A.: A multi-model assessment of pollution transport to the Arctic,
 969 *Atmos. Chem. Phys.*, 8, 5353-5372, doi:10.5194/acp-8-5353-2008, 2008.
- 970 Shindell, D. and Faluvegi, G.: Climate response to regional radiative forcing during the twentieth century, *Nature*
 971 *Geosci.*, 2, 294–300, 2009.
- 972 Skeie, R. B., Berntsen, T., Myhre, G., Pedersen, C. A., Ström, J., Gerland, S., and Ogren, J. A.: Black carbon in the
 973 atmosphere and snow, from pre-industrial times until present, *Atmos. Chem. Phys.*, 11, 6809–6836,
 974 doi:10.5194/acp-11-6809-2011, 2011.
- 975 Stohl, A.: Characteristics of atmospheric transport into the Arctic troposphere, *J. Geophys. Res.-Atmos.*, 111,
 976 D11306, doi:10.1029/2005jd006888, 2006.
- 977 Stohl, A., Klimont, Z., Eckhardt, S., Kupiainen, K., Shevchenko, V. P., Kopeikin, V. M., and Novigatsky, A. N.:
 978 Black carbon in the Arctic: the underestimated role of gas flaring and residential combustion emissions,
 979 *Atmos. Chem. Phys.*, 13, 8833-8855, doi:10.5194/acp-13-8833-2013, 2013.
- 980 [Stohl, A., Aamaas, B., Amann, M., Baker, L. H., Bellouin, N., Berntsen, T. K., Boucher, O., Cherian, R.,](#)
 981 [Collins, W., Daskalakis, N., Dusinska, M., Eckhardt, S., Fuglestad, J. S., Harju, M., Heyes, C.,](#)
 982 [Hodnebrog, Ø., Hao, J., Im, U., Kanakidou, M., Klimont, Z., Kupiainen, K., Law, K. S., Lund, M. T.,](#)
 983 [Maas, R., MacIntosh, C. R., Myhre, G., Myriokefalitakis, S., Olivie, D., Quaas, J., Quennehen, B., Raut, J.-](#)
 984 [C., Rumbold, S. T., Samset, B. H., Schulz, M., Seland, Ø., Shine, K. P., Skeie, R. B., Wang, S., Yttri, K. E.,](#)
 985 [and Zhu, T.: Evaluating the climate and air quality impacts of short-lived pollutants, *Atmos. Chem. Phys.*](#)
 986 [Discuss.](#), 15, 15155-15241, doi:10.5194/acpd-15-15155-2015, 2015.
- 987 VanCuren, R. A.: Asian aerosols in North America: Extracting the chemical composition and mass concentration of
 988 the Asian continental aerosol plume from long-term aerosol records in the western United States, *J.*
 989 *Geophys. Res.*, 108(D20), 4623, doi:10.1029/2003JD003459, 2003.
- 990 van der Werf, G. R., Randerson, J. T., Giglio, L., Collatz, G. J., Mu, M., Kasibhatla, P. S., Morton, D. C.,
 991 DeFries, R. S., Jin, Y., and van Leeuwen, T. T.: Global fire emissions and the contribution of deforestation,
 992 savanna, forest, agricultural, and peat fires (1997–2009), *Atmos. Chem. Phys.*, 10, 11707-11735,
 993 doi:10.5194/acp-10-11707-2010, 2010.

994 Wang, H., Easter, R. C., Rasch, P. J., Wang, M., Liu, X., Ghan, S. J., Qian, Y., Yoon, J.-H., Ma, P.-L., and Vinoj, V.:
995 Sensitivity of remote aerosol distributions to representation of cloud–aerosol interactions in a global
996 climate model, *Geosci. Model Dev.*, 6, 765–782, doi:10.5194/gmd-6-765-2013, 2013.

997 Wang, H., Rasch, P. J., Easter, R. C., Singh, B., Zhang, R., Ma, P. L., Qian, Y., and Beagley, N.: Using an explicit
998 emission tagging method in global modeling of source-receptor relationships for black carbon in the Arctic:
999 Variations, Sources and Transport pathways, *J. Geophys. Res.-Atmos.*, 119, 12888–12909,
1000 doi:10.1002/2014JD022297, 2014.

1001 Wang, M., Xu, B., Cao, J., Tie, X., Wang, H., Zhang, R., Qian, Y., Rasch, P. J., Zhao, S., Wu, G., Zhao, H.,
1002 Joswiak, D. R., Li, J., and Xie, Y.: Carbonaceous aerosols recorded in a southeastern Tibetan glacier:
1003 analysis of temporal variations and model estimates of sources and radiative forcing, *Atmos. Chem. Phys.*,
1004 15, 1191–1204, doi:10.5194/acp-15-1191-2015, 2015.

1005 Wang, Q., Jacob, D. J., Fisher, J. A., Mao, J., Leibensperger, E. M., Carouge, C. C., Le Sager, P., Kondo, Y.,
1006 Jimenez, J. L., Cubison, M. J., and Doherty, S. J.: Sources of carbonaceous aerosols and deposited black
1007 carbon in the Arctic in winter–spring: implications for radiative forcing, *Atmos. Chem. Phys.*, 11, 12453–
1008 12473, doi:10.5194/acp-11-12453-2011, 2011.

1009 Wang, X., S. J. Doherty, and J. Huang: Black carbon and other light-absorbing impurities in snow across Northern
1010 China, *J. Geophys. Res. Atmos.*, 118, 1471–1492, doi:10.1029/2012JD018291, 2013.

1011 Warren, S. G. and Wiscombe, W. J.: A model for the spectral albedo of snow. II: Snow containing atmospheric
1012 aerosols, *J. Atmos. Sci.*, 37, 2734–2745, 1980.

1013 Xu, B., Cao, J., Hansen, J., Yao, T., Joswiak, D. R., Wang, N., Wu, G., Wang, M., Zhao, H., Yang, W., Liu, X., and
1014 He, J.: Black soot and the survival of Tibetan glaciers, *Proc. Natl. Acad. Sci. USA*, 106, 22114–22118,
1015 2009.

1016 Ye, H., Zhang, R., Shi, J., Huang, J., Warren, S. G., and Fu, Q.: Black carbon in seasonal snow across northern
1017 Xinjiang in northwestern China, *Environ. Res. Lett.* 7, 044002, doi:10.1088/1748-9326/7/4/044002, 2012.

1018 Yu, H., Remer, L., Chin, M., Bian, H., Tan, Q., Yuan, T., and Zhang, Y.: Aerosols from Overseas Rival Domestic
1019 Emissions over North America, *Science*, 337, 566–569, 2012.

1020 Yu, H., Chin, M., West, J. J., Atherton, C. S., Bellouin, N., Bergmann, D., Bey, I., Bian, H., Diehl, T., Forberth, G.,
1021 Hess, P., Schulz, M., Shindell, D., Takemura, T., and Tan, Q.: A multimodel assessment of the influence of
1022 regional anthropogenic emission reductions on aerosol direct radiative forcing and the role of
1023 intercontinental transport, *J. Geophys. Res.*, 118, 700–720, doi:10.1029/2012JD018148, 2013.

1024 Zhang, R., Hegg, D. A., Huang, J., and Fu, Q.: Source attribution of insoluble light-absorbing particles in seasonal
1025 snow across northern China, *Atmos. Chem. Phys.*, 13, 6091–6099, doi:10.5194/acp-13-6091-2013, 2013.

1026 Zhang, R., Wang, H., Qian, Y., Rasch, P. J., Easter, R. C., Ma, P.-L., Singh, B., Huang, J., and Fu, Q.: Quantifying
1027 sources, transport, deposition and radiative forcing of black carbon over the Himalayas and Tibetan Plateau,
1028 *Atmos. Chem. Phys. Discuss.*, 15, 77–121, doi:10.5194/acpd-15-77-2015, 2015.

1029 Zhao, C., Hu, Z., Qian, Y., Ruby Leung, L., Huang, J., Huang, M., Jin, J., Flanner, M. G., Zhang, R., Wang, H.,
1030 Yan, H., Lu, Z., and Streets, D. G.: Simulating black carbon and dust and their radiative forcing in seasonal
1031 snow: a case study over North China with field campaign measurements, *Atmos. Chem. Phys.*, 14, 11475–
1032 11491, doi:10.5194/acp-14-11475-2014, 2014.

1033

1034

Table 1. BB and FF fractional contributions based on the PMF and CAM5 source attribution results for BC in snow for each model/observation comparison pair (i). $\overline{C_{obs}^i}$ is the mean of the estimated BC concentrations used in the PMF analysis when more than one sampling sites reside in the same model grid box. $\overline{C_{mod}^i}$ is the JFM mean of CAM5 modeled BC concentrations in snow column. The contributions are calculated as given in Eqs. (A1) (observations) and (A2) (model).

Comparison pair i	$\overline{C_{obs}^i}$ (ng g ⁻¹)	BB_{obs}^i (%)	FF_{obs}^i (%)	$\overline{C_{mod}^i}$ (ng g ⁻¹)	BB_{mod}^i (%)	FF_{mod}^i (%)
1	15.5	62	38	0.8	21	79
2	5.8	100	0	9.5	28	72
3	13.3	51	49	14.7	28	72
4	14.2	70	26	9.8	25	75
5	13.7	47	21	15.3	26	74
6	29.3	27	47	14.3	26	74
7	24.2	27	71	14.2	25	75
8	22.0	20	51	12.6	23	77
9	90.1	0	0	5.4	19	81
10	28.4	16	42	11.3	26	74
11	50.6	7	11	10.1	16	84
12	40.7	11	26	37.1	11	89
13	17.9	34	44	24.0	12	88
14	49.5	23	53	52.5	13	87
15	5.9	46	52	51.8	12	88
16	25.8	16	31	46.6	11	89
17	110.6	3	31	30.5	14	86
18	61.4	8	61	23.3	14	86
19	24.8	13	76	27.6	11	89
20	26.9	17	33	39.9	12	88
21	22.2	26	56	44.5	15	85
22	17.8	31	61	18.2	15	85
23	27.5	23	28	12.6	15	85
24	15.8	22	63	7.2	19	81
25	14.4	32	68	5.6	19	81
26	26.0	0	77	12.6	15	85
27	15.1	15	48	16.0	15	85
28	18.4	16	69	22.0	13	87
29	8.4	66	34	29.2	15	85
30	17.0	18	75	24.8	15	85
31	8.4	45	55	9.1	18	82
32	14.7	30	68	20.2	15	85
33	21.5	24	61	27.3	16	84
34	17.5	18	61	29.8	17	83
35	25.0	22	66	38.9	16	84

HW 8/11/2015 4:12 PM

Deleted: 5

HW 8/11/2015 4:12 PM

Deleted: 6

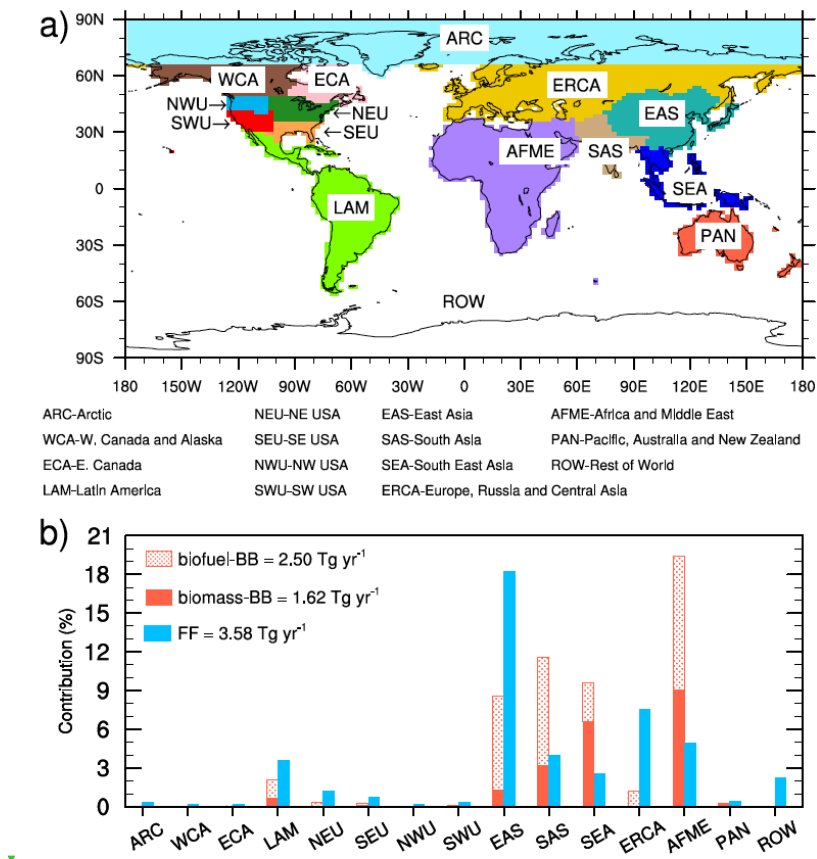
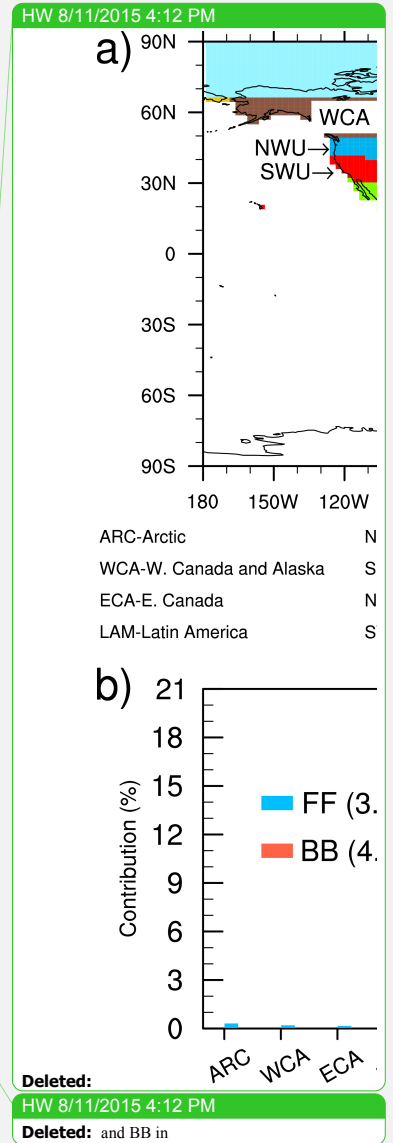


Fig. 1. (a) Tagged source regions and (b) the contributions (%) to the global mean BC emissions (7.69 Tg yr⁻¹) for January, February and March from the individual source regions (marked on the horizontal axis) and sectors (FF in blue, biomass-BB in solid red, and biofuel-BB in dotted red).



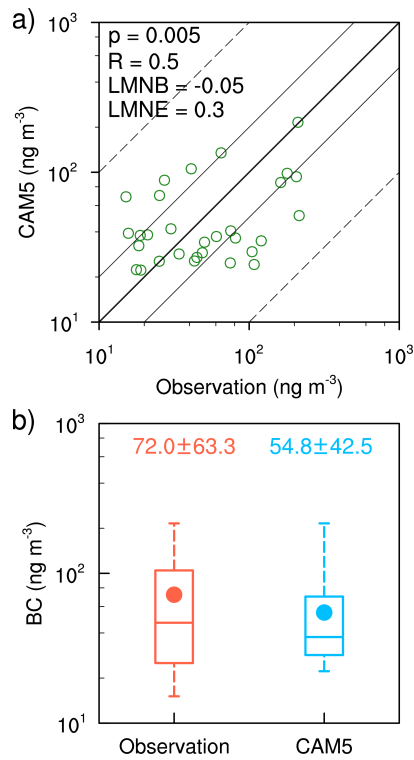


Fig. 2. (a) Scatter plot of CAM5 simulated versus observed JFM mean near-surface atmospheric BC concentrations (ng m^{-3}) in 2013 at the IMPROVE network sites. The observations are averages across sites falling into the same model grid box. The correlation coefficient (R), the statistical significance of R (p), the log-mean normalized bias (LMNB), and the log-mean normalized error (LMNE) are shown in numbers in the top-left corner; the 1:1 (thick solid), 2:1 (thin solid) and 10:1 (dashed) lines are also plotted for reference. (b) Box and whisker plot of observed (red color) and simulated (blue color) JFM mean of near-surface BC concentrations (ng m^{-3}) for all comparison pairs. The 25th, 50th, and 75th percentiles are marked with a box, the mean value with a dot, and the minimum and maximum values with whiskers; the colored numbers give the mean and standard deviation for the observed (red) and modeled values (blue).

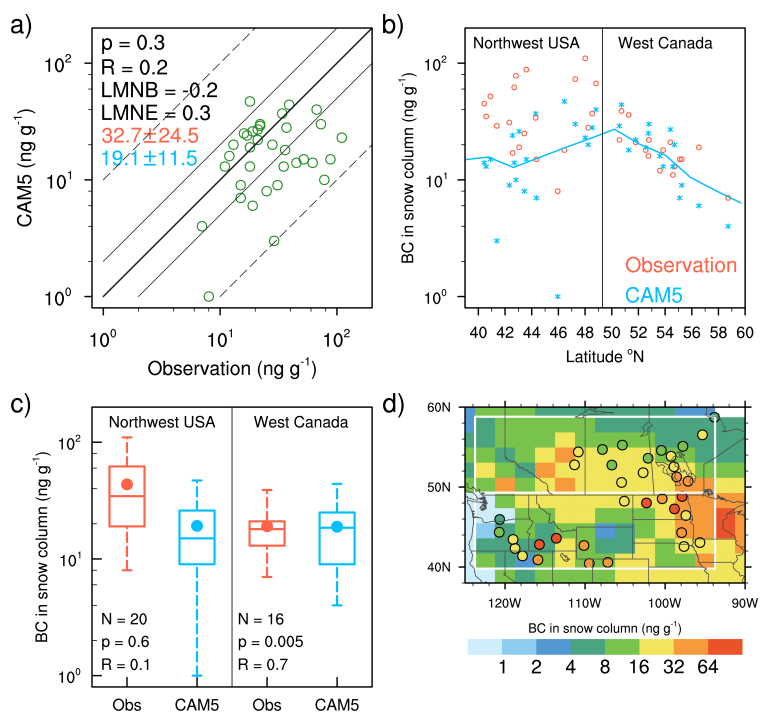


Fig. 3. (a) Scatter plot of simulated versus observed BC concentrations (ng g^{-1}) in the snow column (BCC). As in Figure 2, R , p , LMNB, and LMNE are shown in numbers on the top-left corner; the color numbers show the mean and standard deviation for observations (red) and modeled values (blue). (b) Observed (red circle) and simulated (blue asterisk) BCC versus latitude for the 36 comparison pairs in Northwest USA and West Canada. The modeled values are the JFM mean. The blue line indicates the modeled JFM zonal-mean values over the longitude band $93.75\text{--}123.75^\circ\text{W}$ (white outlines in panel d) for BCC. (c) Box and whisker plot of observed (red color) and simulated (blue color) BCC in the two regions. The 25th, 50th, and 75th percentiles are marked with a box, the mean value with a dot, and the minimum and maximum values with whiskers; the number of samples (N), R , and p for each region are shown at the bottom. (d) Spatial distributions of modeled JFM mean BCC with the observed BCC (color circles with black outlines) superimposed. In d) the observed values are averages across the sampling sites of Doherty et al. (2014), when more than one sampling site fell within a model grid box. The white boxes in d) outline the two receptor regions, Northwest USA ($39.8\text{--}49.3^\circ\text{N}$, $93.75\text{--}123.75^\circ\text{W}$) and West Canada ($49.3\text{--}58.8^\circ\text{N}$, $93.75\text{--}123.75^\circ\text{W}$).

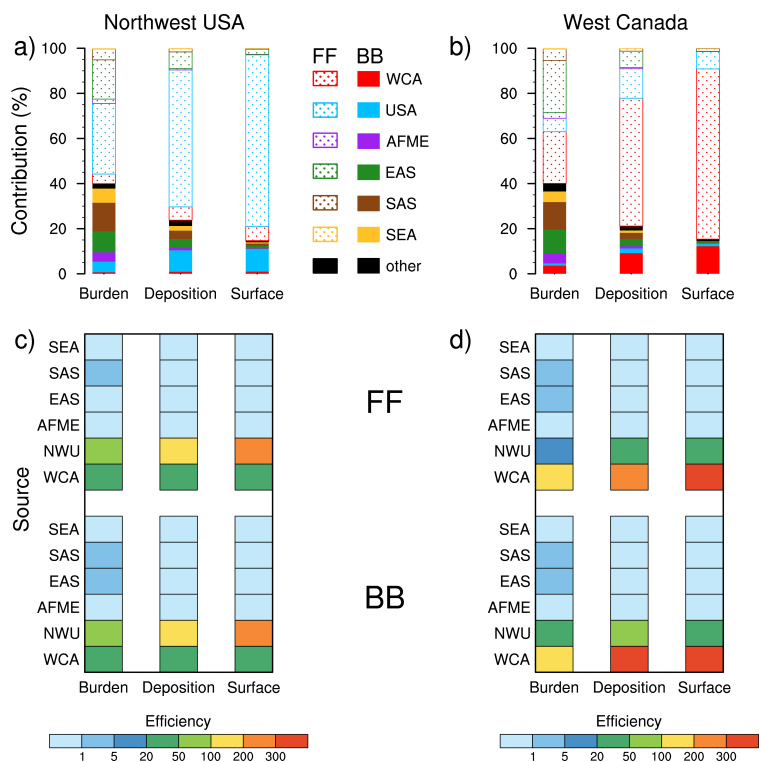


Fig. 4. Fractional contributions to JFM mean BC total column burden, deposition and near-surface concentrations over (a) Northwest USA and (b) West Canada (as defined in Fig. 3d), from six major tagged source regions (colors) and sectors (solid color and stippled bar for BB and FF, respectively); the black bar in each column represents the combined contribution from all of the other tagged source regions and sectors. Panels (c) and (d) show efficiency of FF (top) and BB (bottom) emissions from six major tagged source regions (marked on the y-axis) in changing JFM mean BC total column burden, deposition and near-surface concentrations over Northwest USA (c) and West Canada (d).

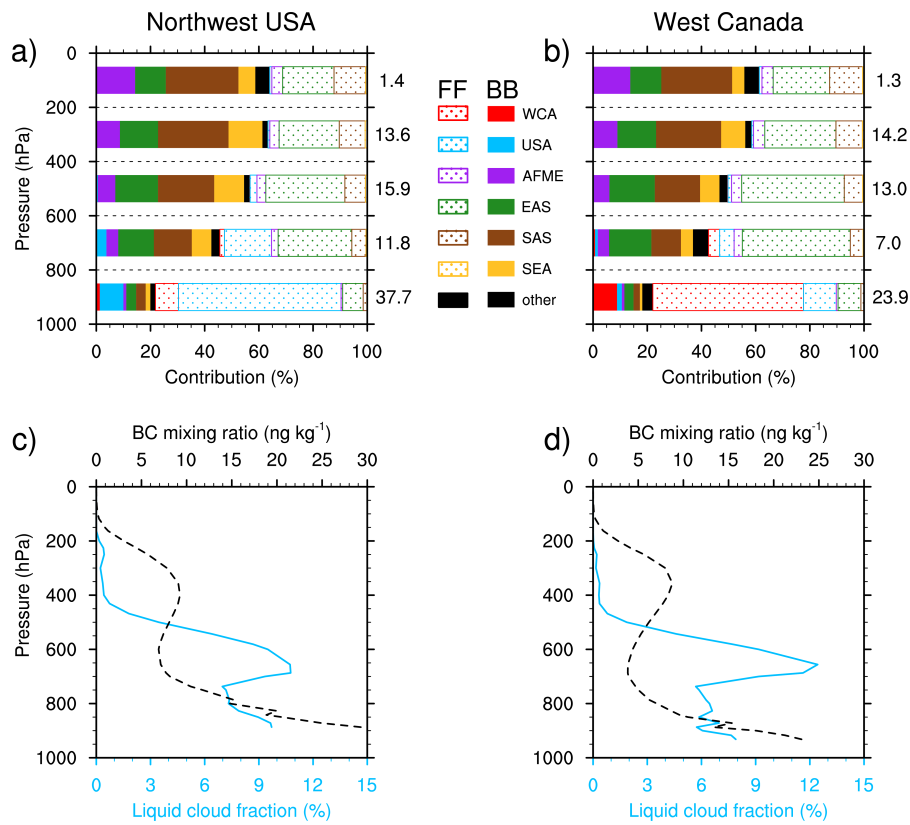


Fig. 5. Panels (a) and (b) are similar to Fig. 4a and b, respectively, but for fractional contributions to BC column burden in five separate vertical layers: 0–200, 200–400, 400–600, 600–800 and 800–1000 hPa. Panels (c) and (d) show the vertical profiles of area-averaged BC mixing ratio (in black) and liquid cloud fraction (in blue) over Northwest USA and West Canada, respectively. All fields are from the CAM5 model run.

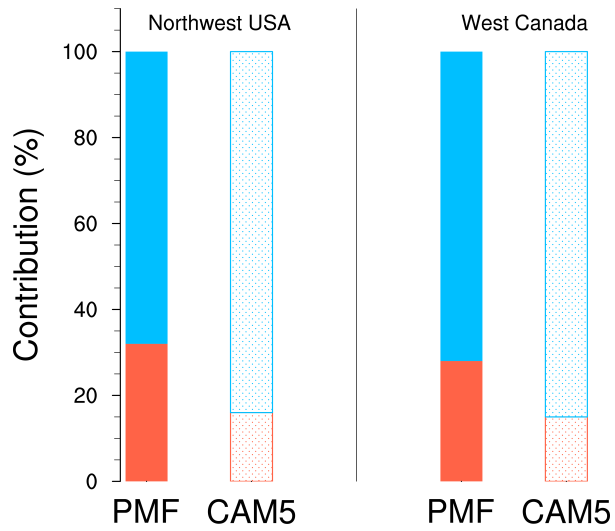


Fig. 6. Regional average contributions from BB (red color) and FF (blue color) sector to combustion-sourced BC in snow in Northwest USA and West Canada based on the PMF analysis (solid bar) and CAM5 simulation (stippled bar). The contributions are calculated as in Eqs. (A3) (observed values) and (A4) (modeled values).

HW 8/11/2015 4:19 PM

Deleted: 7

HW 8/11/2015 4:19 PM

Deleted: 8

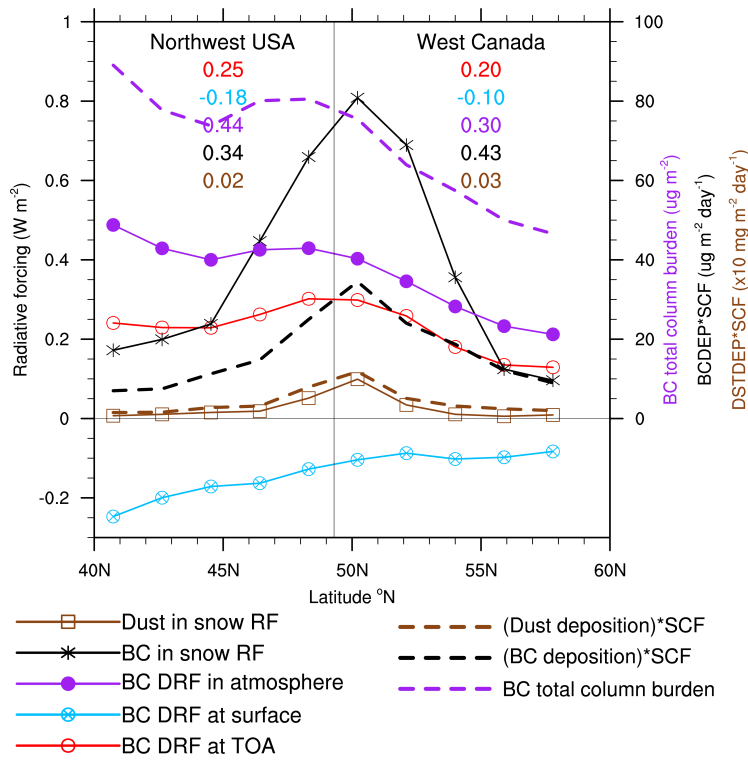


Fig. 7. Modeled JFM and zonal mean radiative forcing (RF) values (in $W m^{-2}$, using y-axis on the left) induced by the various BC effects and the dust-in-snow effect (indicated by the different colors and symbols in the legend) over the longitude band $93.75^{\circ}W$ – $123.75^{\circ}W$ (white outlines in Fig. 3d). The corresponding area-average RF values are shown in colored numbers for Northwest USA and West Canada, respectively. Modeled JFM and zonal mean values of BC total column burden (in $\mu g m^{-2}$), BC deposition (in $\mu g m^{-2} day^{-1}$) and dust deposition (in $10 mg m^{-2} day^{-1}$) multiplied by SCF (snow cover fraction) are shown in colored dashed lines (using y-axis on the right).

Page 13: [1] Moved to page 28 (Move #3) HW 8/11/15 4:12 PM

where $f_{BB}^k + f_{FF}^k + f_{soil}^k = 1$. C_{obs}^k is the estimated snow BC concentrations used in the PMF analysis for the snow sampling site k (Table

Page 13: [2] Deleted HW 8/11/15 4:12 PM

S1). S is the total number of sampling sites within the same model grid box.

Page 13: [3] Deleted HW 8/11/15 4:12 PM

We calculate the average observed snow BC concentrations for all sites within a given

model grid box i , and refer to this as $\overline{C_{obs}^i}$.

In Eq. (6), we calculate the

Page 13: [4] Moved to page 28 (Move #6) HW 8/11/15 4:12 PM

the modeled snow BC concentrations in month j for the model grid box i . D_{BB}^j and D_{FF}^j are fractional

Page 13: [5] Deleted HW 8/11/15 4:12 PM

of BB and FF deposition, respectively, to total BC deposition in month j , and $D_{BB}^j +$

$D_{FF}^j = 1$. M is 3 (total number of months). Note that $BB_{mod}^i + FF_{mod}^i = 1$. Similarly, we

calculate the JFM mean of the modeled BC concentrations in each model grid box i ,

referring to these as $\overline{C_{mod}^i}$.

Page 13: [6] Deleted HW 8/11/15 4:12 PM

(8)

where N is the total number of observation/model comparison pairs (n) in a given region.

Notice that in the denominators of Eq. (7) only the BB_{obs}^n and FF_{obs}^n are included.

